FDTD Analysis of Body Area Communications Using Basic MATLAB Package

S. Makarov and G. Noetscher
ECE Dept., WPI, MA
{makarov,gregn}@wpi.edu

University of Maryland, May 18, 2011
Washington and Northern VA IEEE Chapters

Agenda

- Outline
  - Basic FDTD theory
  - Why MATLAB®?
  - Antenna examples
  - Wireless body area networks (WBANs) and their applications
  - Example of a WBAN network
  - FDTD versus FEM
  - Body models and sensor arrays
  - Continued work

FDTD Theory – Yee grid and material identification

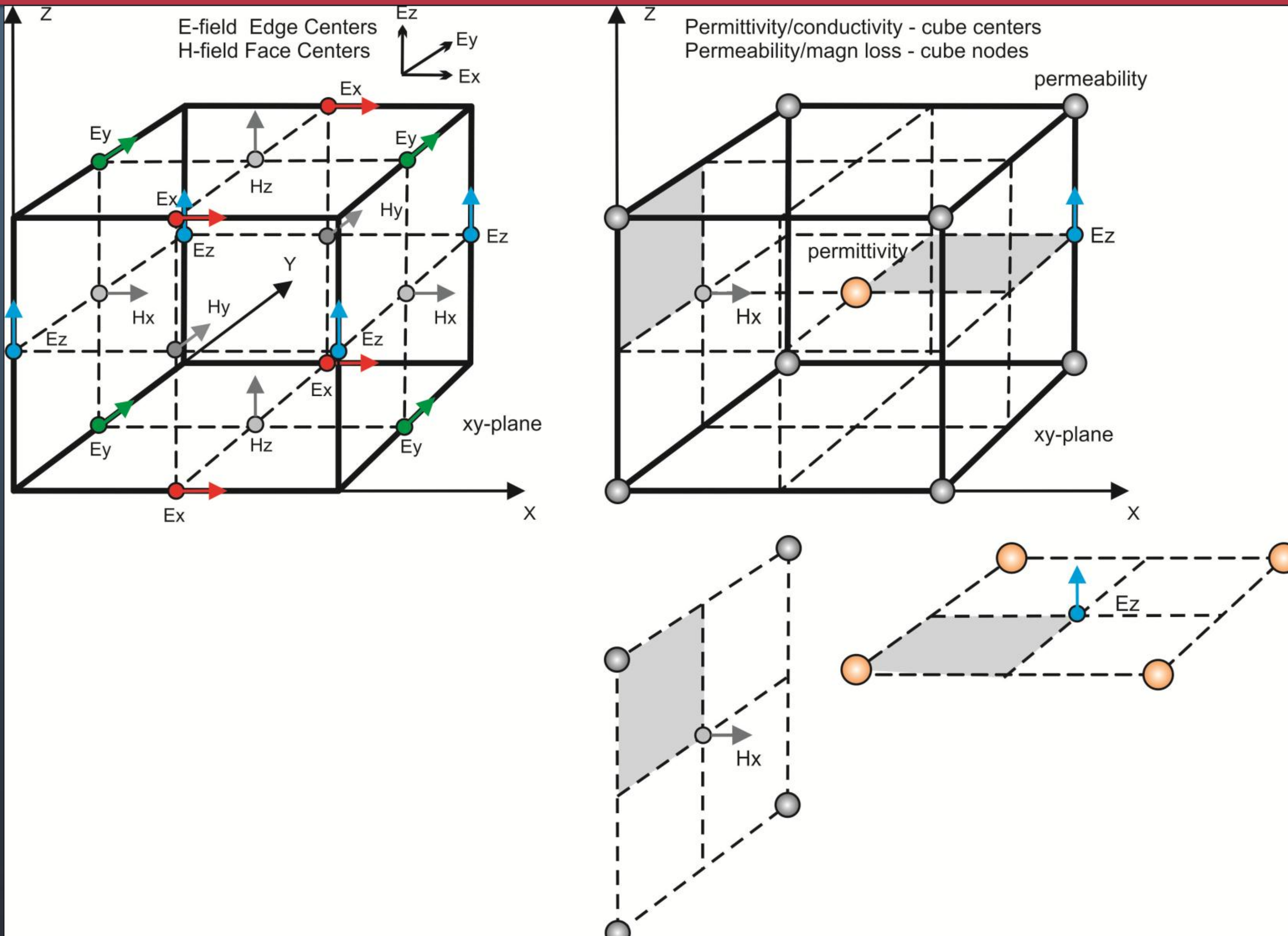

FDTD Theory – Yee grid and material identification (cont.)

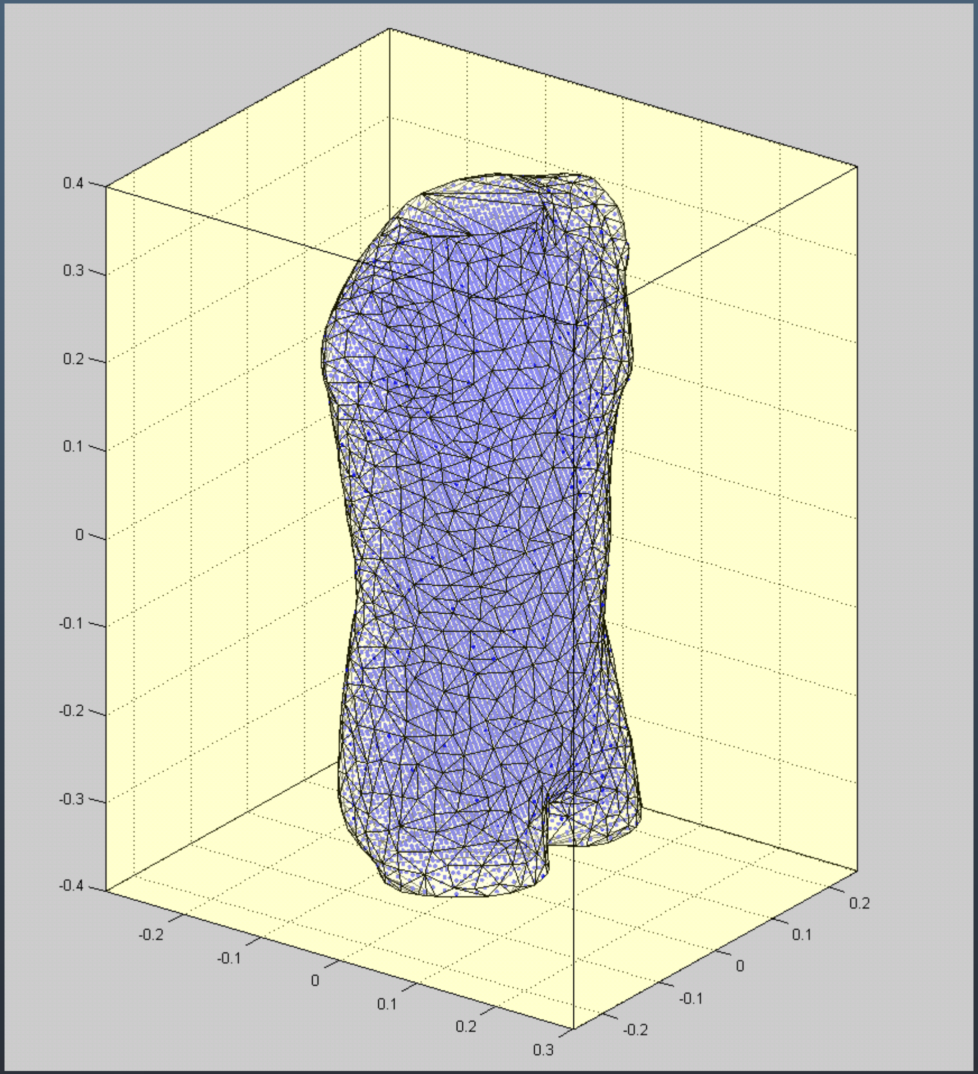

FDTD Theory – assembly of ports and metal/dielectric objects

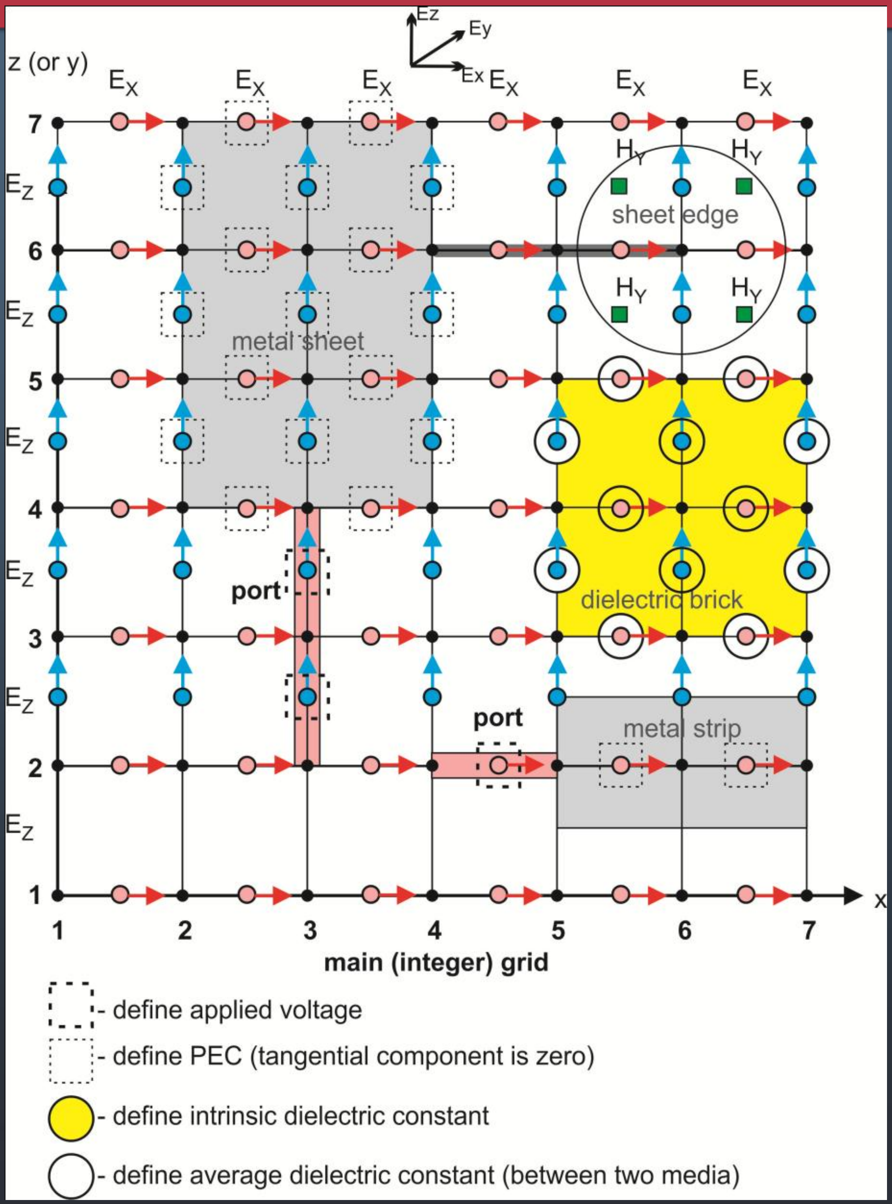

G. Mur, “The modeling of singularities in the finite-difference approximations of the time-domain electromagnetic-field equations,” *IEEE Trans. Microw. Theory Tech., vol. MTT-29, no. 10, pp. 1073–1077,* Oct. 1981.

C. J. Railton, D. L. Paul, I. J. Craddock, and G. S. Hilton, “The Treatment of Geometrically Small Structures in FDTD by the Modification of Assigned Material Parameters,” *IEEE Trans. Antennas Prop., vol. APS-53, no. 12, pp. 4129–4136,* Oct. 1981.

FDTD Theory – port model

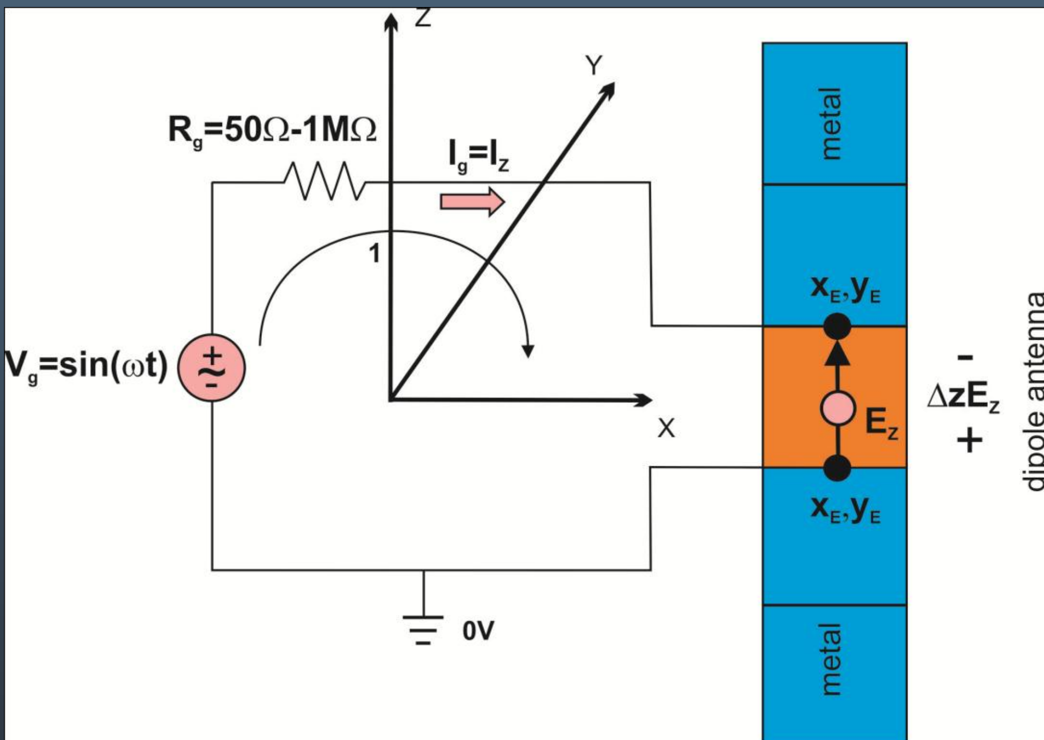

M. Piket-May, A. Taflove, and J. Baron, "FD-TD modeling of digital signal propagation in 3-D circuits with passive and active loads," *IEEE Trans. Microwave Theory and Techniques*, vol. 42, no. 8, Aug. 1994, pp. 1514 - 1523.

$$-V_g(t) + R_g I_g(t) - \Delta z E_z(t, x_e, y_e, z_e) = 0$$

$$I_g(t) = \frac{1}{R_g} V_g(t) + \frac{\Delta z}{R_g} E_z(t, x_e, y_e, z_e)$$

$$\varepsilon \frac{\partial \vec{E}}{\partial t} = \nabla \times \vec{H} - \vec{J}_g$$

FDTD Theory – NFFT

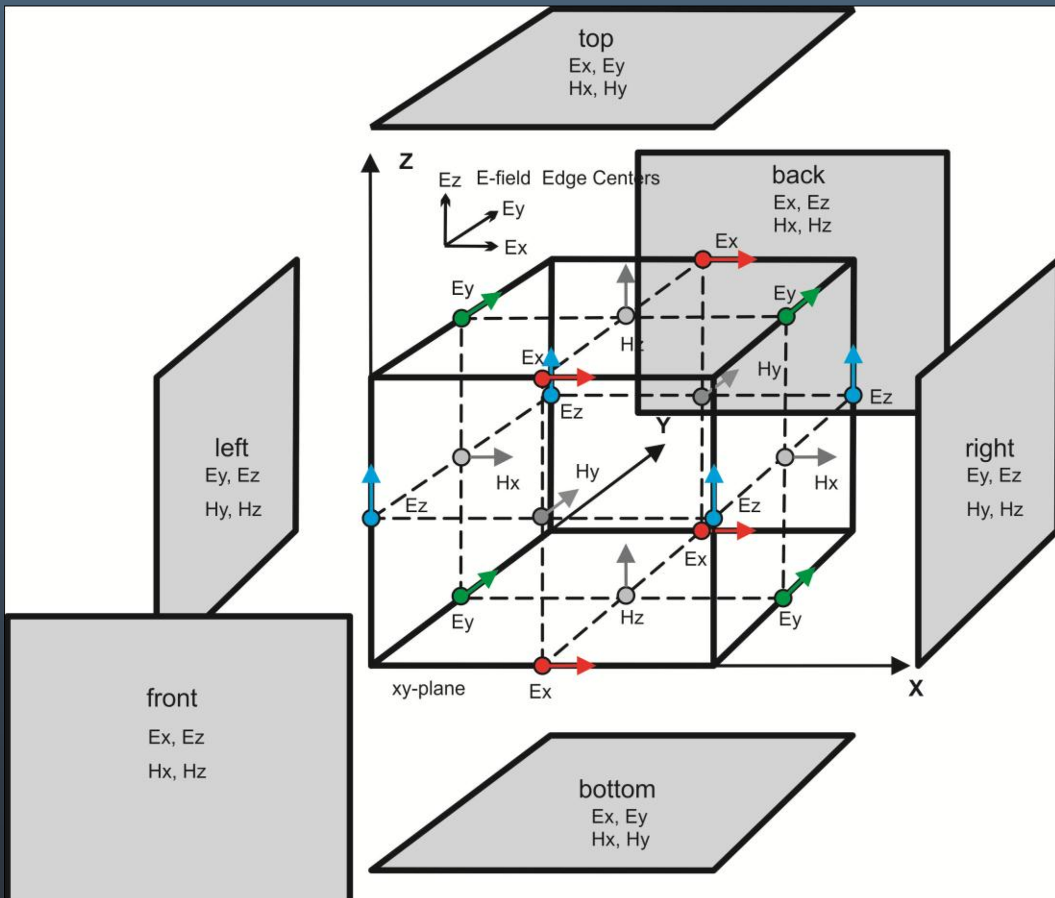

A. Taflove and K. Umashankar, “Radar cross section of general three-dimensional scatterers,” *IEEE Trans. Electromagn. Compat.,* vol. EMC-**25,** no. 4, Nov. 1983**,** pp. 433–440.

FDTD Theory – marching on in time

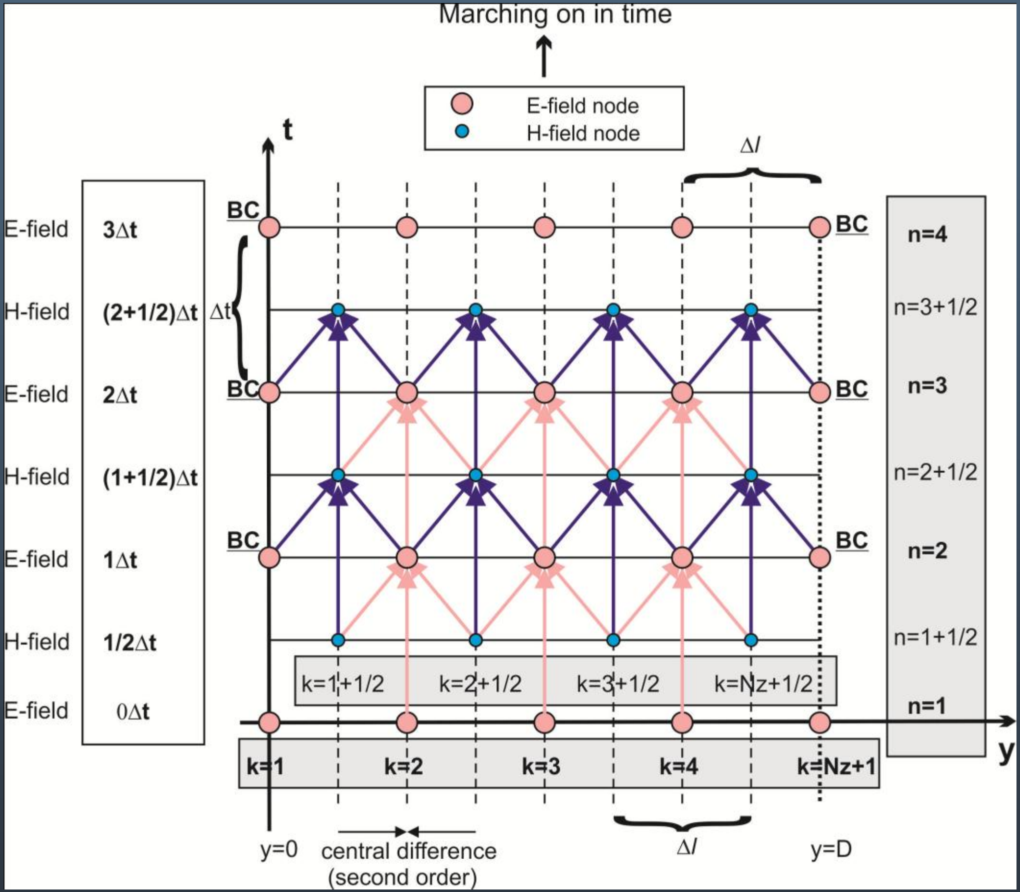

K. S. Yee, "Numerical solution of initial boundary value problem involving Maxwell's equations in isotropic media," *IEEE Trans. Antennas and Propagation*, vol. 14, 1966, pp. 302-307.

$$\varepsilon\frac{\partial E}{\partial t}+\frac{\partial H}{\partial y}=0 \Rightarrow \quad \varepsilon\frac{E_k^{n+1}-E_k^{n}}{\Delta t}+\frac{H_{k+1/2}^{n+1/2}-H_{k-1/2}^{n+1/2}}{\Delta y}=0 \Rightarrow E_k^{n+1}=E_k^{n}-\frac{\Delta t}{\varepsilon\Delta y}(H_{k+1/2}^{n+1/2}-H_{k-1/2}^{n+1/2})$$

$$\mu\frac{\partial H}{\partial t}+\frac{\partial E}{\partial y}=0 \Rightarrow \quad \mu\frac{H_{k+1/2}^{n+3/2}-H_{k+1/2}^{n+1/2}}{\Delta t}+\frac{E_{k+1}^{n+1}-E_k^{n+1}}{\Delta y}=0 \Rightarrow H_{k+1/2}^{n+3/2}=H_{k+1/2}^{n+1/2}-\frac{\Delta t}{\mu\Delta y}(E_{k+1}^{n+1}-E_k^{n+1})$$

FDTD Theory – ABCs/PML

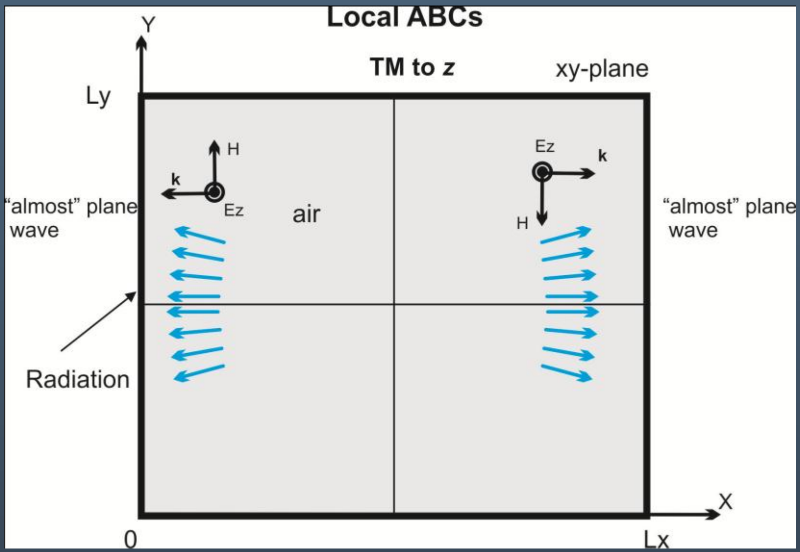

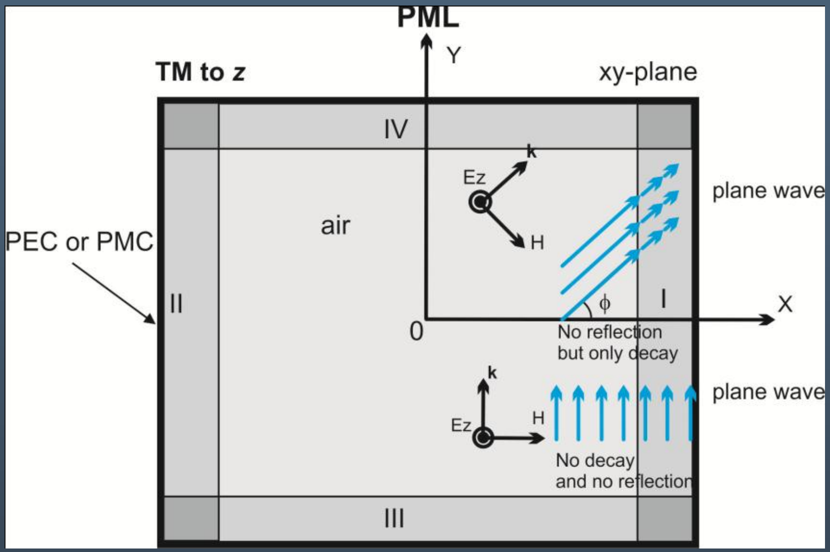

G. Mur, "Absorbing boundary conditions for the finite-difference approximation of the time-domain electromagnetic field equations," *IEEE Trans. Electromagn. Compat.*, vol. EMC-23, no. 4, pp. 377-382, Nov. 1981.

K. K. Mei and J. Fang, "Superabsorption – a method to improve absorbing boundary conditions," *IEEE Trans. Antennas and Propagation*, vol. 40, no. 9, Sep. 1992, pp. 1001-1010.

J.-P. Bérenger, "A perfectly matched layer for the absorption of electromagnetic waves," *J. Comput. Phys.*, vol. 114, pp. 185–200, Oct. 1994.

J.-P. Bérenger, "Three-dimensional perfectly matched layer for the absorption of electromagnetic waves," *J. Comput. Phys.*, vol. 127, pp. 363–379, 1996.

FDTD Theory – putting it all together - 1D propagation

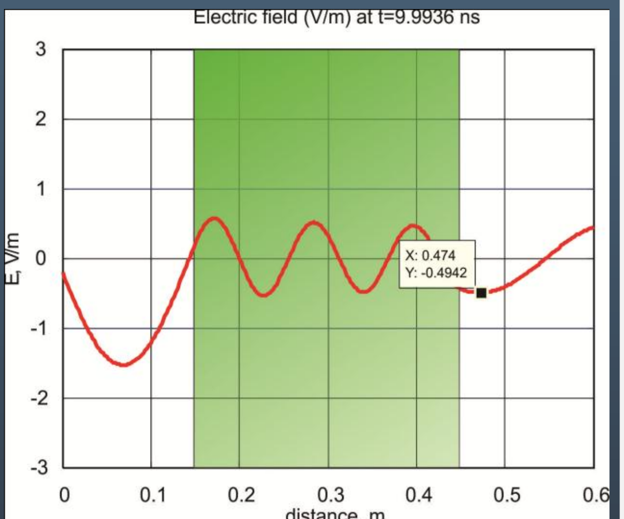


```
%--------------------------------------------------------------------
%   Electric field source and impedance boundary conditions
f = 1e9;                          %  Frequency of interest
Eleft  = 2*sin(2*pi*f*t);         %  Electric field source, left
Eright = 0*sin(2*pi*f*t);         %  Electric field source, right
Rleft  = eta;                     %  Surface impedance, left boundary
Rright = eta;                     %  Surface impedance, right boundary

B1inv   =  1/(Rleft*epsilon/delta + 1);      %     BC coefficient -left
B1dir   =    (Rleft*epsilon/delta - 1);      %     BC coefficient -left
B2inv   =  1/(Rright*epsilon/delta + 1);     %     BC coefficient -right
B2dir   =    (Rright*epsilon/delta - 1);     %     BC coefficient -right

e1      = (1 - dt*sig_profile./(2*eps_profile))./...
          (1 + dt*sig_profile./(2*eps_profile));
e2      = (dt./(dl*eps_profile))./...
          (1 + dt*sig_profile./(2*eps_profile));
h1       = 1;
h2       = dt/(dl*mu);

%   Main loop - "bootstrapping"
n = 1;
while n <= NT-1
    Enext(1)    = B1inv*( B1dir*Epast(1)    - 2*Rleft*Hpast(1)   + Eleft(n)  +Eleft(n+1));
    Enext(Nl+1)= B2inv*( B2dir*Epast(Nl+1)+ 2*Rright*Hpast(Nl)+ Eright(n)+Eright(n+1));

    Enext(indv)  = e1(indv).*Epast(indv)  - e2(indv).*(Hpast(indv+0)  - Hpast(indv-1));
    Hnext(indi)  = h1*       Hpast(indi)  - h2*       (Enext(indi+1)  - Enext(indi-0));
    Epast = Enext; Hpast = Hnext; n = n + 1;
end
```

$$\varepsilon\frac{\partial E}{\partial t}+\frac{\partial H}{\partial y}-\sigma E=0 \Rightarrow \quad \varepsilon\frac{E_k^{n+1}-E_k^n}{\Delta t}+\frac{H_{k+1/2}^{n+1/2}-H_{k-1/2}^{n+1/2}}{\Delta y}-\sigma\frac{E_k^{n+1}+E_k^n}{2}=0$$

$$\mu\frac{\partial H}{\partial t}+\frac{\partial E}{\partial y}=0 \Rightarrow \quad \mu\frac{H_{k+1/2}^{n+3/2}-H_{k+1/2}^{n+1/2}}{\Delta t}+\frac{E_{k+1}^{n+1}-E_k^{n+1}}{\Delta y}-\sigma^*\frac{H_{k+1/2}^{n+3/2}+H_{k+1/2}^{n+1/2}}{2}=0$$

Resonant effects (Mr. Xu Yang)

$$Q = \omega \frac{W}{P_d} = \frac{\omega \varepsilon_r \varepsilon_0}{\sigma_e}$$

- Using average body properties of 0.5 S/m
  - Permittivity of 40, Q is **1.79**
  - Permittivity of 50, Q is **2.24**
- Results are for lowest TM mode

Why MATLAB®?

- Simple coding:

```
%%  E-field update (everywhere except on the boundary, 45% of CPU time)
    ExN(:,2:Ny,2:Nz) = Ex1.*ExP(:,2:Ny,2:Nz) + Ex2.*(diff(HzP(:,:,2:Nz),1,2) -
diff(HyP(:,2:Ny,:),1,3));
    EyN(2:Nx,:,2:Nz) = Ey1.*EyP(2:Nx,:,2:Nz) + Ey2.*(diff(HxP(2:Nx,:,:),1,3) -
diff(HzP(:,:,2:Nz),1,1));
    EzN(2:Nx,2:Ny,:) = Ez1.*EzP(2:Nx,2:Ny,:) + Ez2.*(diff(HyP(:,2:Ny,:),1,1) -
diff(HxP(2:Nx,:,:),1,2));
%%  H-field update (everywhere, 35% of CPU time)
            HxN =  Hx1.*HxP + Hx2.*(diff(EyN,1,3)- diff(EzN,1,2));
            HyN =  Hy1.*HyP + Hy2.*(diff(EzN,1,1)- diff(ExN,1,3));
            HzN =  Hz1.*HzP + Hz2.*(diff(ExN,1,2)- diff(EyN,1,1));
```

- Parallel processor support
- Flexibility
- Simple geometry generation/import
- Low cost
- “Seeing” the fields

Antenna examples

- Patch antennas

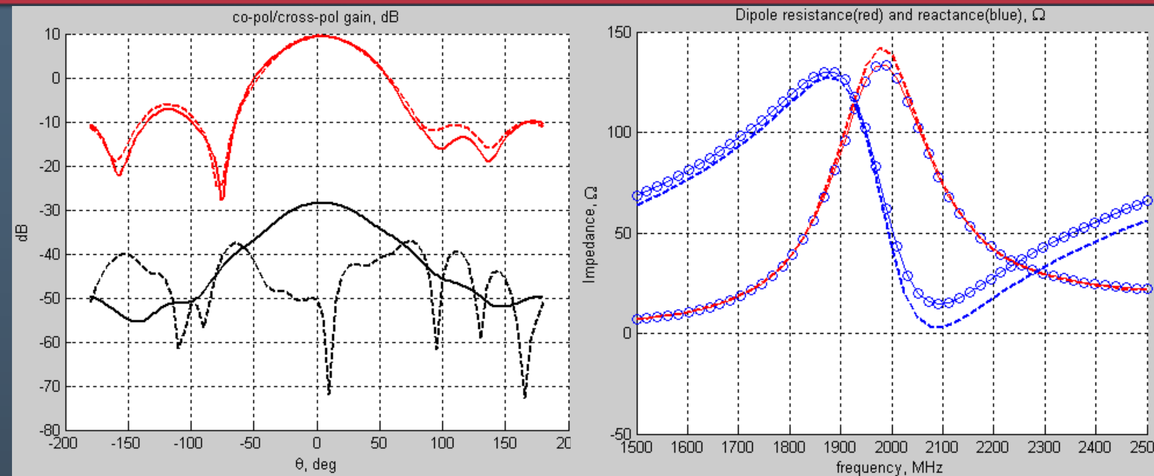

- Antenna arrays

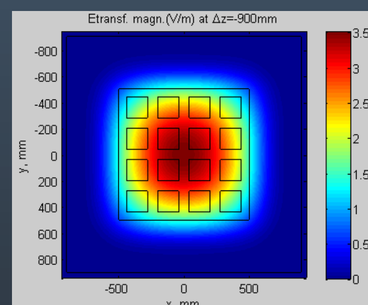

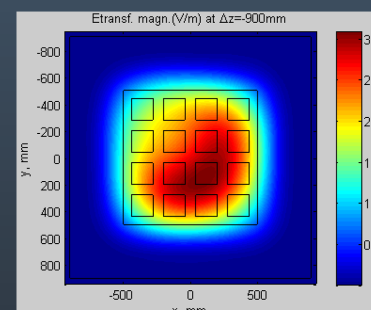

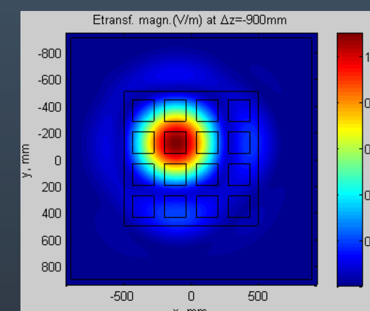

- Simple MIMO arrangements

WBANs and their applications

- Wireless Body Area Networks (WBANs) require reliable communication channels
  - Many antenna types/configurations
  - Path loss must be characterized accurately
- Military, medical and commercial applications
  - Wearable antennas
  - Out-patient sensor networks
  - Medical sensor in-plants
- FCC establishment of Medical Device Radio Communications Service at 401-406 MHz

Use FDTD in WBANs

M. J. Burfeindt, E. Zastrow, S. C. Hagness, B. D. Van Veen, and J. E. Medow, “Microwave beamforming for non-invasive patient-specific hyperthermia treatment of pediatric brain cancer,” Phys. Med. Biol. **56** (2011) 2743–2754.

M. Converse, E. J. Bond, B. D. Van Veen, and S. C. Hagness, “A Computational Study of Ultra-Wideband Versus Narrowband Microwave Hyperthermia for Breast Cancer Treatment,” *IEEE Trans. Microw. Theory Tech.*, vol. 54, no. 5, pp. 2169–2180, May 2006.

H. Terchoune, D. Lautru, A. Gati, A.C. Carrasco, M.F. Wong, J. Wiart, V.F. Hanna, “On-body Radio Channel Modeling for Different Human Body Models Using FDTD Techniques,” *Microwave and Optical Technology Letters*, Vol. 51, No. 10, pp 2498-2501, October 2009.

M. Slegban, S. Mazur, C. Törnevik, “Comparisons of Measurements and FDTD Calculations of Mobile Phone Electromagnetic Far-Fields and Near-Fields,” *Antennas and Propagation Society International Symposium*, Montreal, July 1997.

W.G. Scanlon, N.E. Evans, "Numerical analysis of bodyworn UHF antenna systems," *Electronics & Communication Engineering Journal*, pp. 55-64, April 2001.

J.N. Bringuier, R. Mittra, J. Wiart, “Efficient Modeling of Body Area Networks using the Parallized FDTD, it's Serial Parallel Extension and the Time Domain Green's Function Method,” *The 2nd European Conference on Antennas and Propagation*, pp. 1-5, 2007.

Example of a WBAN network

- Both Tx and Rx are modeled by **out–of-body** small dipole co-polar antennas terminated to a 50 Ω series resistance
- Single frequency of 402 MHz
- Voltage/power transfer function is evaluated

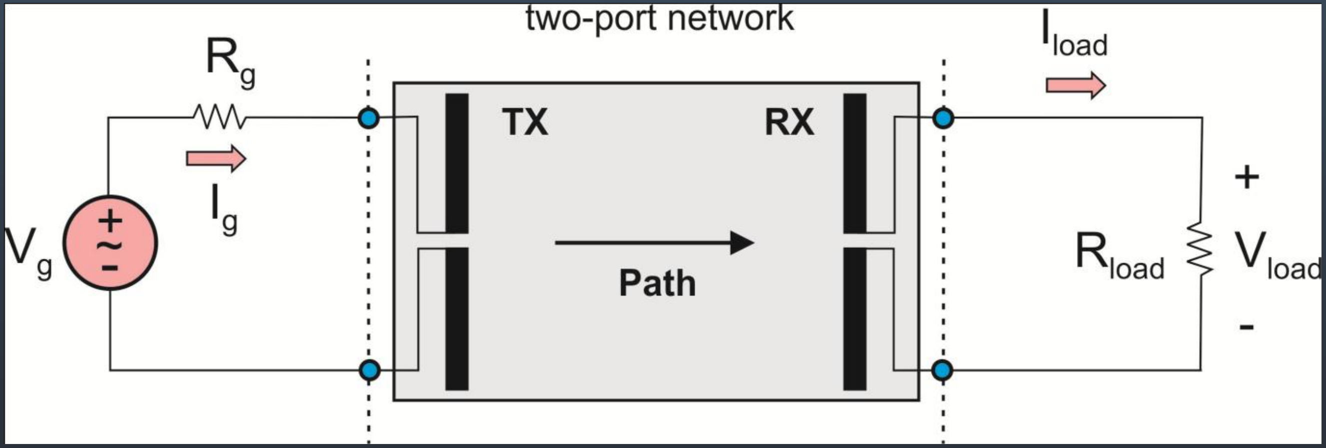

$$T_V = \frac{V_{load}}{V_g}$$

$$T_V = \frac{1}{2} S_{21}$$

Our task

- Compare performance of MATLAB FDTD and FEM simulator Ansoft/ANSYS HFSS
- Establish how important the effect of internal body composition is on the performance of wireless link
- Establish how important the effect of body shape variation is on the performance of wireless link

Non-homogeneous Ansoft/ANSYS mesh – FEM simulator

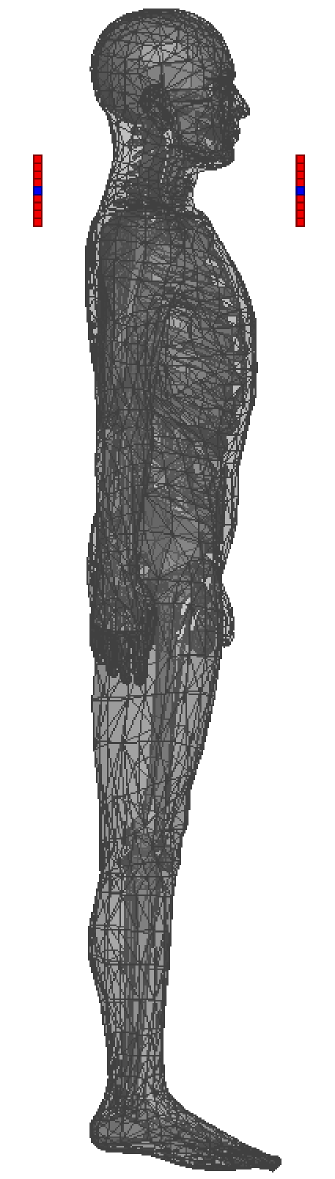

- Constructed of over 300 separate parts
  - 2mm resolution
  - individual electrical properties
- Perfectly Matched Layer (PML) boundary conditions
- Simulated in Ansoft/ANSYS HFSS via FEM
- Scattering parameters found directly

Homogenous mesh – FDTD simulator

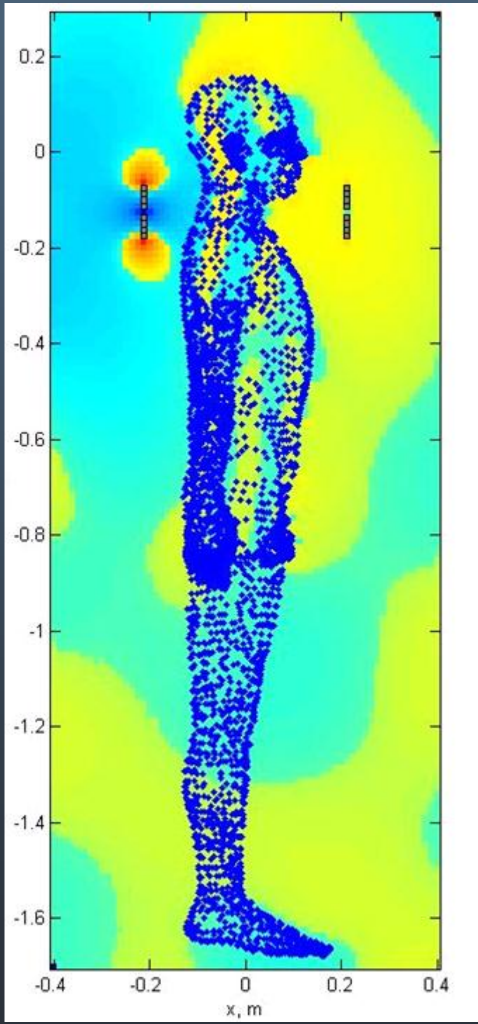

- One equivalent homogenous body model
  - – Rel. dielectric constant of 50
  - – Conductivity of 0.5 S/m
- Simulation domain of 310,000 brick elements coded in MATALB
- Mur ABCs
- Voltage TF is evaluated

Simulation results

Case 04_01:
Antenna position: X = 206.5mm, Z = -130.5mm.

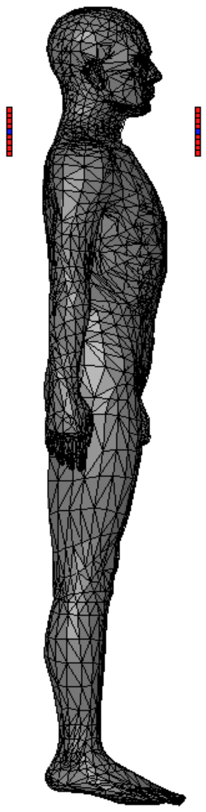

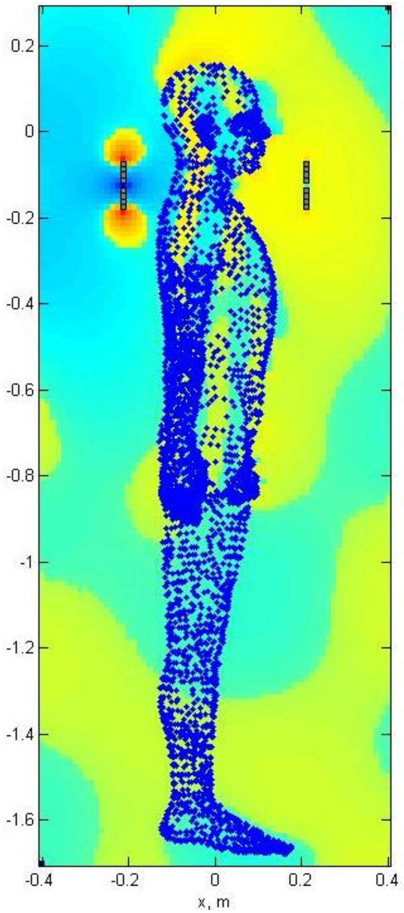

Adaptive Step Mesh Size (elements)	Z-matrix, Ω	S-Matrix	Received voltage amplitude, mV Ansoft/ANSYS (top) FDTD (bottom)	ANSOFT Runtime (HH:MM:SS)
1 388,240	Z_{11} = 86-88.1° Z_{22} = 170.8-87.7° Z_{21} = 0.499-167°	S_{11} = 0.97111 -60.3° S_{22} = 0.9782-32.6° S_{21} = 2.75e-3 -36.9°	**1.4** **0.119**	01:18:19
2 465,892	Z_{11} = 236.47-89.1° Z_{22} = 327.1-88.7° Z_{21} = 0.4686-171°	S_{11} = 0.99347 -23.9° S_{22} = 0.99312-17.4° S_{21} = 5.821e-4 -13.5°	**0.291** **0.119**	02:56:47
3 559,074	Z_{11} = 397.68-89.4° Z_{22} = 425.97-89.1° Z_{21} = 0.48-171°	S_{11} = 0.99724 -14.5° S_{22} = 0.99619-13.4° S_{21} = 2.825e-4 -6.11°	**0.139** **0.119**	05:41:02
4 670,892	Z_{11} = 448.5-89.5° Z_{22} = 462.2-89.2° Z_{21} = 0.464-170°	S_{11} = 0.99789 -12.7° S_{22} = 0.99697-12.3° S_{21} = 2.206e-4 -4.37°	**0.11** **0.119**	10:30:06
5 805,074	Z_{11} = 474.4-89.5° Z_{22} = 477.4-89.2° Z_{21} = 0.4498-170°	S_{11} = 0.99818 -12° S_{22} = 0.99724-12° S_{21} = 1.96e-4 -3.65°	**0.098** **0.119**	15:19:00
6 966,089	Z_{11} = 483.3-89.5° Z_{22} = 484.8-89.3° Z_{21} = 0.4447-170°	S_{11} = 0.99826 -11.8° S_{22} = 0.99737-11.8° S_{21} = 1.874e-4 -3.38°	**0.0937** **0.119**	20:14:30
7 1,074,751	Z_{11} = 489.59-89.5° Z_{22} = 488.2-89.3° Z_{21} = 0.4425-170°	S_{11} = 0.9983 -11.7° S_{22} = 0.99742-11.7° S_{21} = 1.835e-4 -3.24°	**0.0914** **0.119**	27:09:30
8 1,141,585	Z_{11} = 489.6-89.5° Z_{22} = 490.1-89.3° Z_{21} = 0.441-170°	S_{11} = 0.9983 -11.7° S_{22} = 0.99745-11.6° S_{21} = 1.816e-4 -3.18°	**0.0908** **0.119**	23:29:10

Simulation results (cont'd.)

Case 04_02:

Antenna position: X = 206.5mm, Z = -190.5mm.

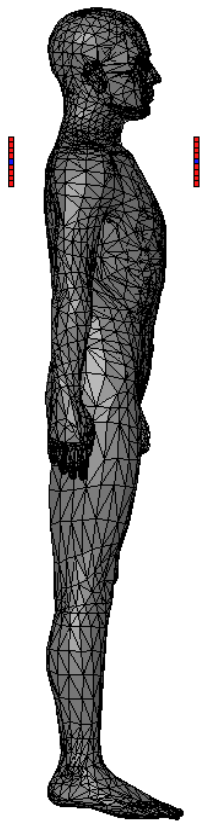

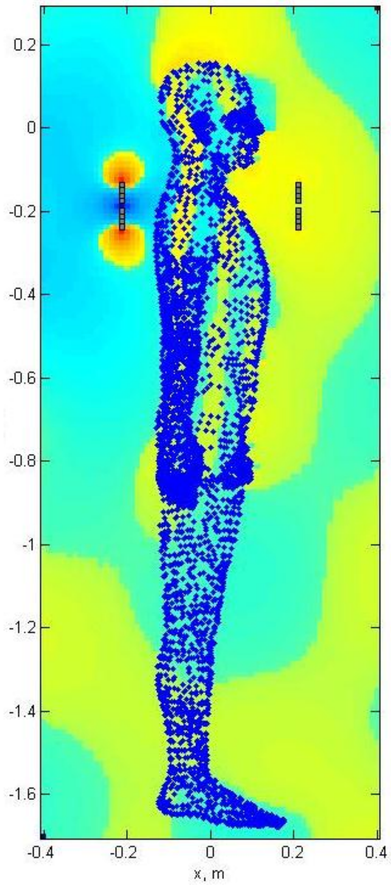

Adaptive Step Mesh Size (elements)	Z-matrix, Ω	S-Matrix	Received voltage amplitude, mV Ansoft/ANSYS (top) FDTD (bottom)	ANSOFT Runtime (HH:MM:SS)
1 388,089	Z_{11} = 106.7-88.1° Z_{22} = 54.8-88.4° Z_{21} = 0.208 166°	S_{11} = 0.9753 -50.2° S_{22} = 0.97288-84.7° S_{21} = 2.316e-3 -83.7°	**1.2** **0.09**	01:09:17
2 465,709	Z_{11} = 287.8-89.4° Z_{22} = 180.45-88.8° Z_{21} = 0.2555 168°	S_{11} = 0.9963 -19.7° S_{22} = 0.9896-31° S_{21} = 4.638e-4 -39.2°	**0.232** **0.09**	02:31:47
3 558,855	Z_{11} = 394.7-89.5° Z_{22} = 354.7-89.1° Z_{21} = 0.3348 169°	S_{11} = 0.9977 -14.4° S_{22} = 0.9957-16° S_{21} = 2.341e-4 -27.6°	**0.117** **0.09**	05:15:30
4 670,631	Z_{11} = 449.5-89.5° Z_{22} = 440-89.2° Z_{21} = 0.3517 169°	S_{11} = 0.9982 -12.7° S_{22} = 0.997-13° S_{21} = 1.7518e-4 -25	**0.0876** **0.09**	10:37:06
5 804,762	Z_{11} = 471.5-89.6° Z_{22} = 470.4-89.3° Z_{21} = 0.3468 169°	S_{11} = 0.9984 -12.1° S_{22} = 0.9974-12.1° S_{21} = 1.5431e-4 -24.1°	**0.0772** **0.09**	17:58:02
6 964,718	Z_{11} = 481.3-89.6° Z_{22} = 482-89.3° Z_{21} = 0.343 169°	S_{11} = 0.9985 -12.1° S_{22} = 0.9975-12.1° S_{21} = 1.4598e-4 -24.1°	**0.073** **0.09**	22:26:22
7 1,054,674	Z_{11} = 486.7 -89.6° Z_{22} = 487.1-89.3° Z_{21} = 0.3406169 °	S_{11} = 0.9985 -11.7° S_{22} = 0.9976-11.7° S_{21} = 1.419e-4-23.6°	**0.071** **0.09**	24:53:08
8	**Matrix Solve Exception: Failed**		 **0.09**	

Simulation results (cont'd.)

Case 04_03:

Antenna position: X = 206.5mm, Z = -390.5mm.

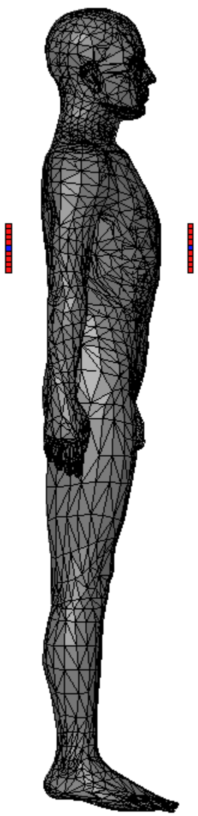

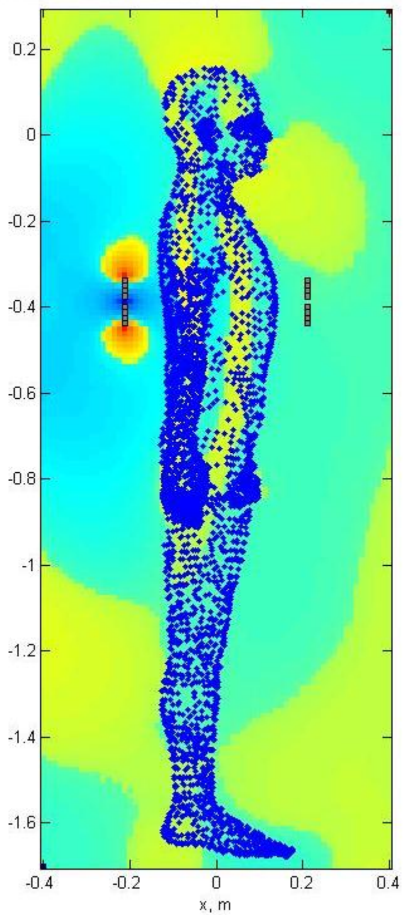

Adaptive Step Mesh Size (elements)	Z-matrix, Ω	S-Matrix	Received voltage amplitude, mV Ansoft/ANSYS (top) FDTD (bottom)	ANSOFT Runtime (HH:MM:SS)
1 400,358	Z_{11} = 156.6-88.3° Z_{22} = 95.86-87.9° Z_{21} = 0.072-32.6°	S_{11} = 0.98264 -35.4° S_{22} = 0.96984-55.1° S_{21} = 3.95e-4 98.9°	**0.1975** **0.008**	01:41:35
2 480,430	Z_{11} = 308.1-89.2° Z_{22} = 264.2-89.3° Z_{21} = 0.061-35.1°	S_{11} = 0.99543 -18.4° S_{22} = 0.99556-21.4° S_{21} = 7.291e-5 123°	**0.0362** **0.008**	03:09:06
3 576,520	Z_{11} = 417.9-89.4° Z_{22} = 405.4-89.5° Z_{21} = 0.059-35°	S_{11} = 0.99773 -13.6° S_{22} = 0.99792-14.1° S_{21} = 3.441e-5 130°	**0.0171** **0.008**	06:38:42
4 691,827	Z_{11} = 455.0-89.5° Z_{22} = 454.5-89.6° Z_{21} = 0.0563-35.1°	S_{11} = 0.99819 -12.5° S_{22} = 0.99844-12.6° S_{21} = 2.684e-5 132°	**0.0134** **0.008**	10:49:25
5 830,194	Z_{11} = 473.6-89.6° Z_{22} = 473.8-89.6° Z_{21} = 0.0546-34.7°	S_{11} = 0.9984 -12.1° S_{22} = 0.9986-12° S_{21} = 2.4e-5 132°	**0.012** **0.008**	13:43:17
6 996,235	Z_{11} = 482.5-89.6° Z_{22} = 482.6-89.6° Z_{21} = 0.0538-34.7°	S_{11} = 0.9985 -11.8° S_{22} = 0.9987 -11.8° S_{21} = 2.281e-5 133°	**0.011** **0.008**	22:12:00
7 1,130,503	Z_{11} = 486.9-89.6° Z_{22} = 487-89.6° Z_{21} = 0.0533-34.7°	S_{11} = 0.9985 -11.7° S_{22} = 0.9987 -11.7° S_{21} = 2.221e-5133°	**0.011** **0.008**	22:08:02
8 1,250,345	Z_{11} = 489.4-89.6° Z_{22} = 489.35-89.6° Z_{21} = 0.0531-34.7 °	S_{11} = 0.9986-11.7° S_{22} = 0.9987-11.7° S_{21} = 2.1896e-5133°	**0.011** **0.008**	27:55:01

Simulation results (cont'd.)

Case 04_04:
Antenna position: X = 306.5mm, Z = -390.5mm.

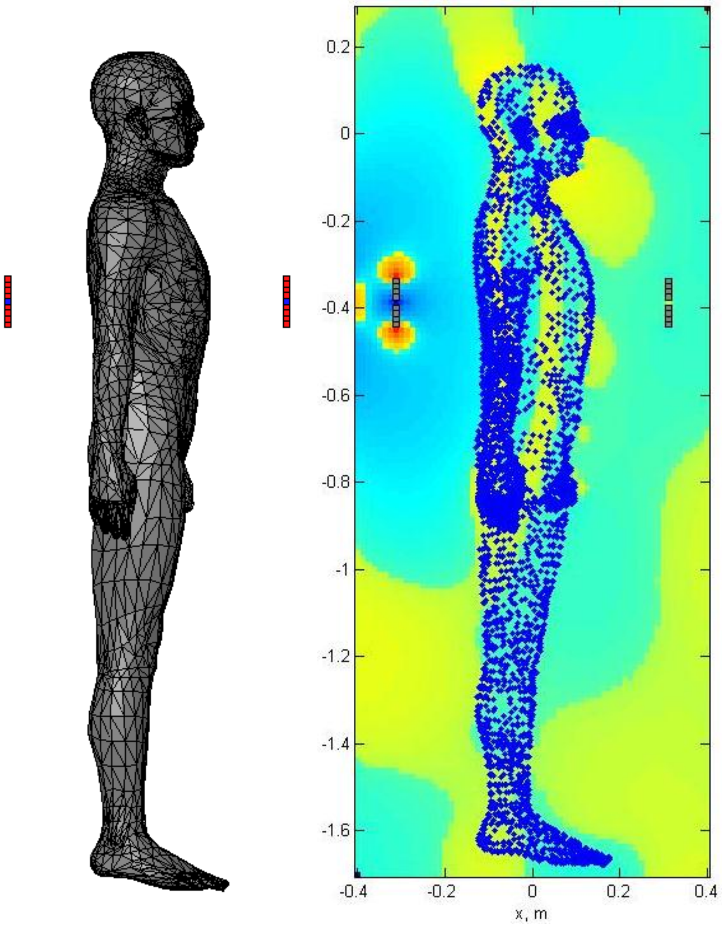

Adaptive Step Mesh Size (elements)	Z-matrix, Ω	S-Matrix	Received voltage amplitude, mV Ansoft/ANSYS (top) FDTD (bottom)	ANSOFT Runtime (HH:MM:SS)
1 400,142	Z_{11} = 68.6-85.7° Z_{22} = 56.3-80.9° Z_{21} = 0.164-10.9°	S_{11} = 0.9304 -72.1° S_{22} = 0.85301-83.1° S_{21} = 2.2958e-3 - 83.6°	**1.2** **0.0223**	01:02:58
2 480,173	Z_{11} = 164.7-88.0° Z_{22} = 229.0-88.1° Z_{21} = 0.135 6.3°	S_{11} = 0.9805 -33.8° S_{22} = 0.98599 -24.6° S_{21} = 3.2975e-4 153°	**0.165** **0.0223**	02:56:59
3 576,213	Z_{11} = 345.9-88.9° Z_{22} = 397.4-89.1° Z_{21} = 0.127 8.25°	S_{11} = 0.99435 -16.4° S_{22} = 0.99623-14.3° S_{21} = 9.0199e-5 171°	**0.045** **0.0223**	07:05:07
4 691,457	Z_{11} = 433.7-88.2° Z_{22} = 451.4-89.3° Z_{21} = 0.112 7.65°	S_{11} = 0.99675 -13.2 ° S_{22} = 0.99732-12.6° S_{21} = 5.6095e-5 173°	**0.028** **0.0223**	12:33:51
5 829,750	Z_{11} = 466.8-89.3° Z_{22} = 474.1-89.4° Z_{21} = 0.107 7.7°	S_{11} = 0.9973 -12.2° S_{22} = 0.99769-12° S_{21} = 4.7411e-5 174°	**0.024** **0.0223**	16:46:48
6 995,703	Z_{11} = 480.7-89.3° Z_{22} = 483.9-89.4° Z_{21} = 0.105 7.75°	S_{11} = 0.9975-11.9° S_{22} = 0.9978-11.8° S_{21} = 4.4255e-5175°	**0.022** **0.0223**	21:00:35
7 1,088,680	Z_{11} = 486.7-89.3° Z_{22} = 488.5-89.4° Z_{21} = 0.103 7.76°	S_{11} = 0.9975 -11.9° S_{22} = 0.9978-11.8° S_{21} = 4.426e-5 175°	**0.021** **0.0223**	24:23:31
8 1,226,879	Z_{11} = 489.8-89.3° Z_{22} = 490.9-89.4° Z_{21} = 0.103 7.77°	S_{11} = 0.9977 -11.7° S_{22} = 0.9979-11.6° S_{21} = 4.227e-5 175°	**0.021** **0.0223**	29:32:16

Simulation results (cont'd.)

Case 04_05:
Antenna position: X = 156.5mm, Z = -390.5mm.

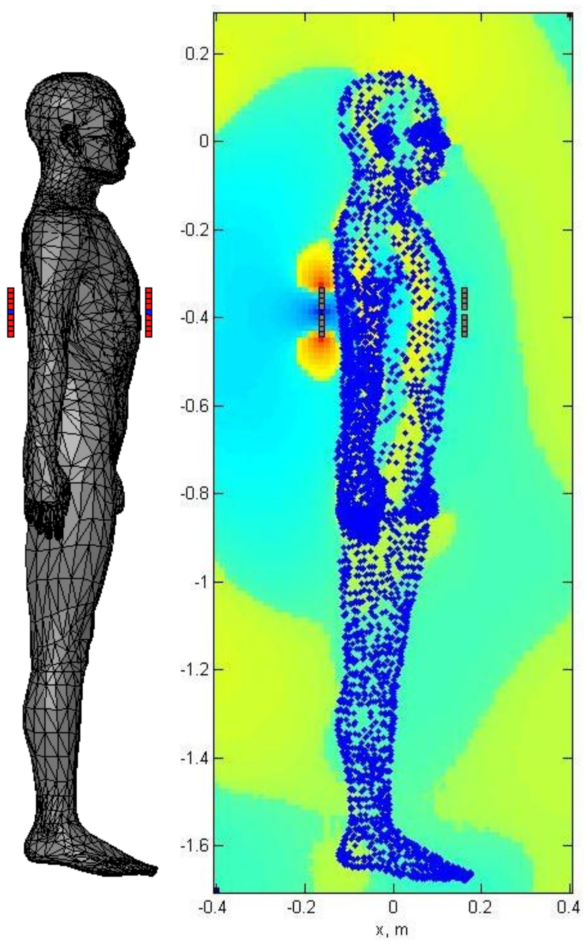

Adaptive Step Mesh Size (elements)	Z-matrix, Ω	S-Matrix	Received voltage amplitude, mV Ansoft/ANSYS (top) FDTD (bottom)	ANSOFT Runtime (HH:MM:SS)
1 400,193	Z_{11} = 165.8-88° Z_{22} = 226.3-88.2° Z_{21} = 0.171-29.3°	S_{11} = 0.981 -33.5° S_{22} = 0.9872-24.9° S_{21} = 4.187e-4 118°	**0.21** **0.0349**	01:10:16
2 480,239	Z_{11} = 319.4-89° Z_{22} = 356.7-88.8° Z_{21} = 0.161-25°	S_{11} = 0.9947 -17.8° S_{22} = 0.9945-16° S_{21} = 1.378e-4 136°	**0.069** **0.0349**	02:46:16
3 576,290	Z_{11} = 418.4-89.2° Z_{22} = 415.2-89° Z_{21} = 0.156-23.5°	S_{11} = 0.9969 -13.6° S_{22} = 0.996-13.7° S_{21} = 8.8249e-5 141°	**0.044** **0.0349**	05:05:49
4 691,549	Z_{11} = 451.98-89.3° Z_{22} = 436.8-89.1° Z_{21} = 0.151-23.1°	S_{11} = 0.9974 -12.6° S_{22} = 0.9964-13.1° S_{21} = 7.5194e-5 143°	**0.038** **0.0349**	08:19:50
5 829,863	Z_{11} = 465.7-89.4° Z_{22} = 446.2-89.1° Z_{21} = 0.148-23°	S_{11} = 0.9976 -12.3° S_{22} = 0.9966-12.8° S_{21} = 7.0322e-5 143°	**0.035** **0.0349**	12:26:51
6 995,836	Z_{11} = 472.2-89.4° Z_{22} = 451.5-89.1° Z_{21} = 0.147-22.9°	S_{11} = 0.9977 -12.1° S_{22} = 0.9967-12.6° S_{21} = 6.7928e-5 143°	**0.034** **0.0349**	17:21:15
7 1,134,472	Z_{11} = 475.5-89.4° Z_{22} = 454.2-89.1° Z_{21} = 0.146-22.9°	S_{11} = 0.9978 -12° S_{22} = 0.9968-12.6° S_{21} = 6.675e-5143°	**0.033** **0.0349**	25:49:41
8 1,361,367	Z_{11} = 477.3-89.4° Z_{22} = 455.7-89.1° Z_{21} = 0.146-22.9°	S_{11} = 0.9978 -12° S_{22} = 0.9968-12.5° S_{21} = 6.6123e-5 143°	**0.033** **0.0349**	27:57:15

Simulation results (cont’d.)

Case 04_06:
Antenna position: X = 146.5mm, Z = -390.5mm.

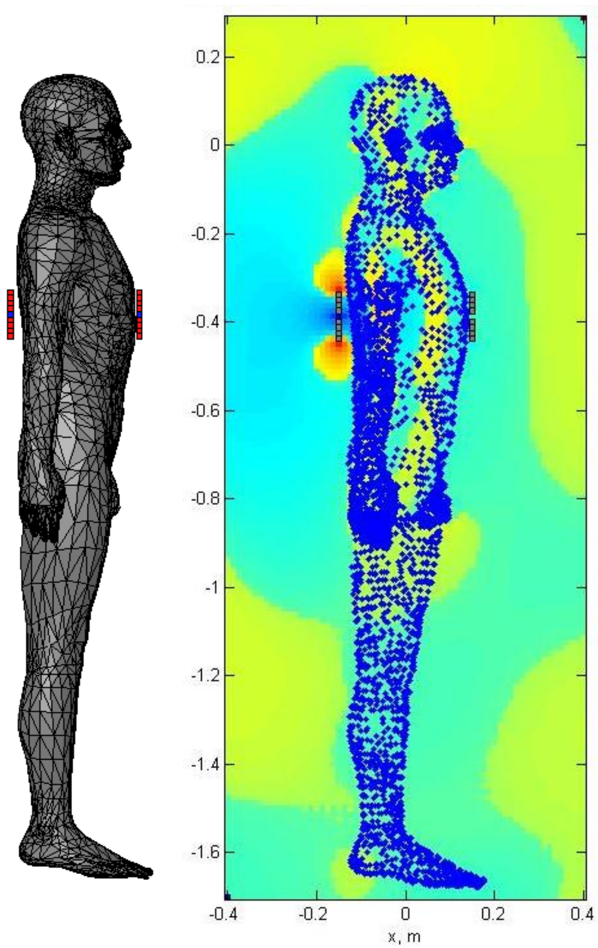

Adaptive Step Mesh Size (elements)	Z-matrix, Ω	S-Matrix	Received voltage amplitude, mV Ansoft/ANSYS (top) FDTD (bottom)	ANSOFT Runtime (HH:MM:SS)
1 400,328	Z_{11} = 192.7-88.5° Z_{22} = 219.8-87.3° Z_{21} = 0.174-14.9°	S_{11} = 0.987 -29.1° S_{22} = 0.9796-25.6° S_{21} = 3.8133e-4 154°	**0.191** **0.0581**	01:09:04
2 480,422	Z_{11} = 350.8-88.7° Z_{22} = 328.8-88° Z_{21} = 0.207-11.4°	S_{11} = 0.9939 -16.2° S_{22} = 0.9899-17.3° S_{21} = 1.741e-4 149°	**0.087** **0.0581**	02:58:32
3 576,510	Z_{11} = 414.5-89° Z_{22} = 371.4-88.2° Z_{21} = 0.202-10.2°	S_{11} = 0.9957 -13.8° S_{22} = 0.9919-15.3° S_{21} = 1.28e-4 153°	**0.063** **0.0581**	04:52:22
4 691,815	Z_{11} = 441.1-89.1° Z_{22} = 388.3-88.3° Z_{21} = 0.196-9.8°	S_{11} = 0.9963 -12.9° S_{22} = 0.9926-14.7° S_{21} = 1.124e-4 154°	**0.056** **0.0581**	08:11:20
5 830,184	Z_{11} = 451.4-89.1° Z_{22} = 395.6-88.4° Z_{21} = 0.194-9.8°	S_{11} = 0.9965 -12.6° S_{22} = 0.9929-14.4° S_{21} = 1.0678e-4 154°	**0.053** **0.0581**	11:19:46
6 996,227	Z_{11} = 456.8-89.1° Z_{22} = 399.5-88.4° Z_{21} = 0.193-9.7°	S_{11} = 0.9967 -12.5° S_{22} = 0.9931-14.3° S_{21} = 1.0401e-4 154°	**0.052** **0.0581**	15:19:59
7 1,179,976	Z_{11} = 459.4-89.1° Z_{22} = 401.4-88.4° Z_{21} = 0.193-9.63°	S_{11} = 0.9967 -12.4° S_{22} = 0.9932-14.2° S_{21} = 1.0266e-4 155°	**0.051** **0.0581**	20:58:45
8 1,280,114	Z_{11} = 460.7-89.1° Z_{22} = 402.4-88.4° Z_{21} = 0.193-9.62°	S_{11} = 0.9967 -12.4° S_{22} = 0.9932-14.2° S_{21} = 1.0199e-4 155°	**0.051** **0.0581**	25:08:17

Simulation results (cont'd.)

Case 04_07:
Antenna position: X = 356.5mm, Z = -390.5mm.

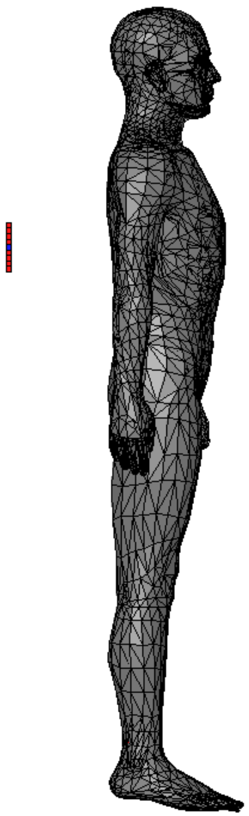

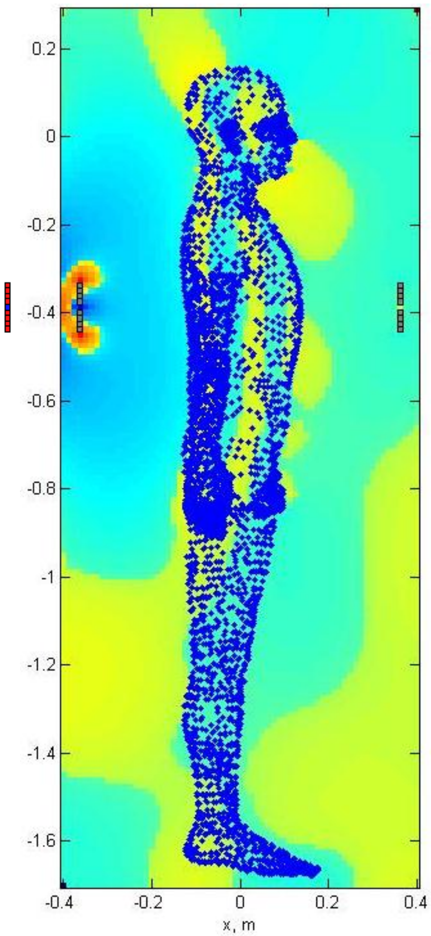

Adaptive Step Mesh Size (elements)	Z-matrix, Ω	S-Matrix	Received voltage amplitude, mV Ansoft/ANSYS (top) FDTD (bottom)	ANSOFT Runtime (HH:MM:SS)
1 399,884	Z_{11} = 51.76-83.3° Z_{22} = 75-84.5° Z_{21} = 0.186-25.7°	S_{11} = 0.8893 -88° S_{22} = 0.9149-67.3° S_{21} = 2.5955e-3 69.3°	**1.3** **0.0246**	01:11:38
2 479,861	Z_{11} = 134.2-87.5° Z_{22} = 209-87.9° Z_{21} = 0.153-21.6°	S_{11} = 0.9721 -40.9° S_{22} = 0.9838-26.9° S_{21} = 4.854e-4 120°	**0.243** **0.0246**	03:12:03
3 575,834	Z_{11} = 328.2-88.7° Z_{22} = 377.5-88.9° Z_{21} = 0.166-18.3°	S_{11} = 0.9932 -17.3° S_{22} = 0.9952-15.1° S_{21} = 1.3037e-4 143°	**0.063** **0.0246**	07:24:23
4 691,003	Z_{11} = 423-89° Z_{22} = 444.9-89.2° Z_{21} = 0.152-17.7°	S_{11} = 0.996 -13.5° S_{22} = 0.9969-12.8° S_{21} = 7.961e-5 147°	**0.04** **0.0246**	12:41:40
5 829,204	Z_{11} = 463.7-89.2° Z_{22} = 473-89.3° Z_{21} = 0.142-17.7°	S_{11} = 0.997 -12.3° S_{22} = 0.9974-12.1° S_{21} = 6.3895e-5 149°	**0.032** **0.0246**	16:49:03
6 995,047	Z_{11} = 479.8-89.2° Z_{22} = 483.7-89.3° Z_{21} = 0.138-17.8°	S_{11} = 0.9973 -11.9° S_{22} = 0.9977-11.8° S_{21} = 5.879e-5 149°	**0.029** **0.0246**	21:27:27
7 1,102,183	Z_{11} = 486.9-89.3° Z_{22} = 488.9-89.3° Z_{21} = 0.136-17.8°	S_{11} = 0.9974 -11.7° S_{22} = 0.9977-11.7° S_{21} = 5.655e-5 149°	**0.028** **0.0246**	24:56:38
8 1,164,687	Z_{11} = 490.4-89.3° Z_{22} = 491.2-89.3° Z_{21} = 0.136-17.8°	S_{11} = 0.99746 -12.4° S_{22} = 0.9977-14.2° S_{21} = 5.556e-5 155°	**0.028** **0.0246**	25:47:53

Relative error comparison

Case Number	Estimated Relative Error of Received Voltage (%) : FDTD vs. the finest FEM mesh $\delta = \frac{\lvert \upsilon_{HFSS} - \upsilon_{FDTD} \rvert}{\upsilon_{HFSS}} \times 100$	Ansoft/ANSYS HFSS Runtime (HH:MM:SS)	FDTD Runtime (MM:SS)
1	23.7	23:29:10	10:57
2	21.1	24:53:08	15:22
3	27	27:55:01	28:01
4	6.19	29:32:16	28:12
5	5.76	27:57:15	27:51
6	13.9	25:08:17	15:12
7	12.1	25:47:53	27:45

Testing different body shapes

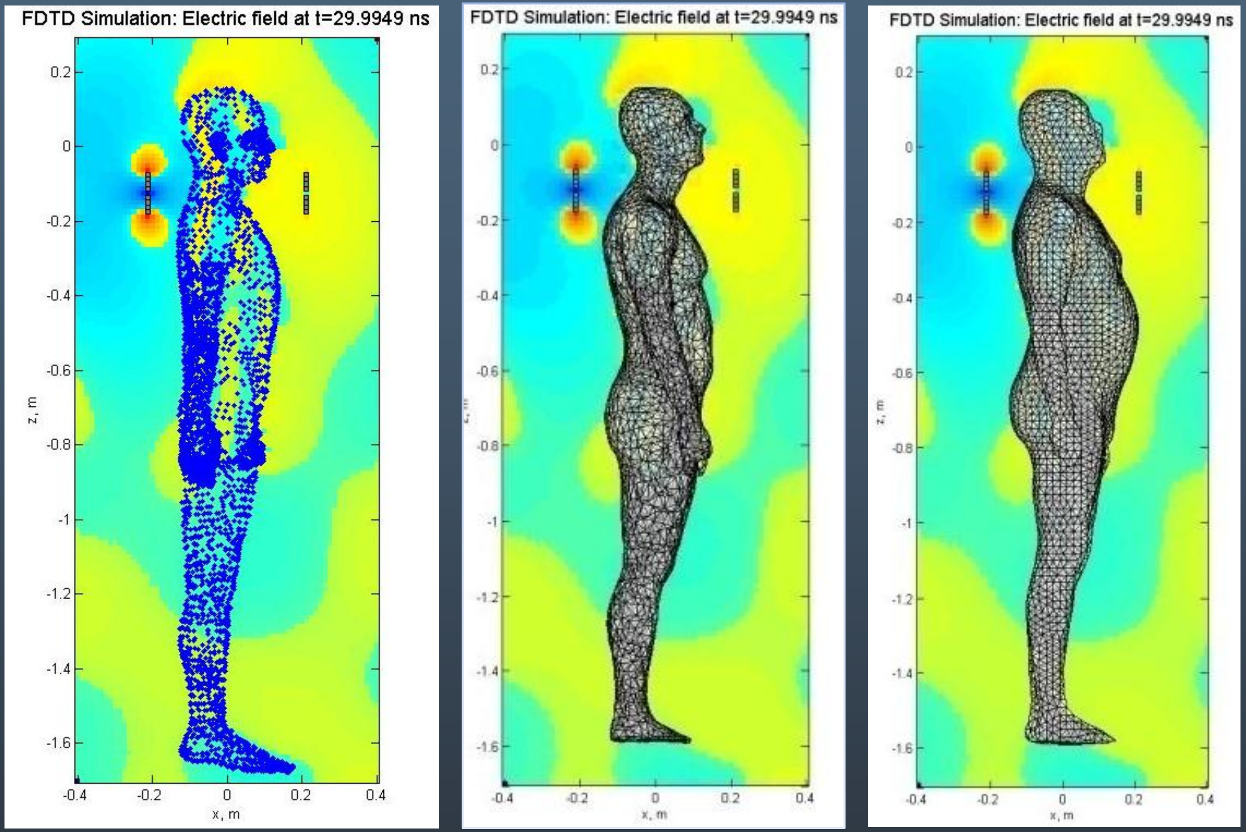

Case Designation	Received Voltage (mV)
WPI Male A	0.119
WPI Male B	0.119
Ansys Mesh	0.119

Conclusions for out-of-body networks at 402 MHz

- Performed code-to-code validation
- Established that FDTD is superior to FEM w.r.t. CPU time
- Established that:
  - Out-of-body wireless link weakly depends on internal body composition
  - Out-of-body wireless link weakly depends on body shape
  - Critical diffraction parameters include path length and body area projected onto the plane perpendicular to path

Body models: custom mesh creation

- Surface meshes for four human volunteer body models were created using a 3D scanner at U.S. Army Natick Soldier Research, Development and Engineering Center

- Manufactured by Cyberware, the Whole Body Color 3D Scanner, Model WB4, can acquire shape and color of the entire body in a single pass and output a variety of digital formats.
- More info is available at the company website: http://www.cyberware.com/products/scanners/wb4.html

Mesh manipulation

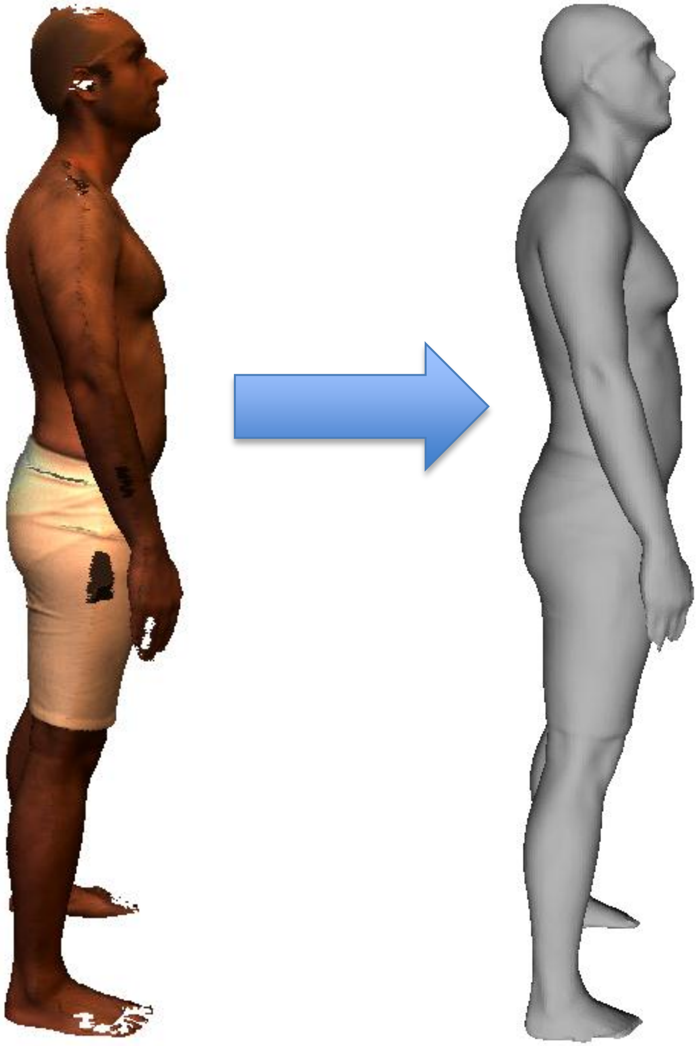

- Meshlab is an open source tool used for mesh manipulation. Capabilities include:
  - Variety of import and export formats
  - Surface mesh construction
  - Patching of surface voids
  - Mesh smoothing
  - http://meshlab.sourceforge.net

FDTD implementation

- Uniform 3D FDTD grid constructed
- Cell centers tested – if inside mesh manifold, electrical constants modified
- FDTD solution of Maxwell's equations

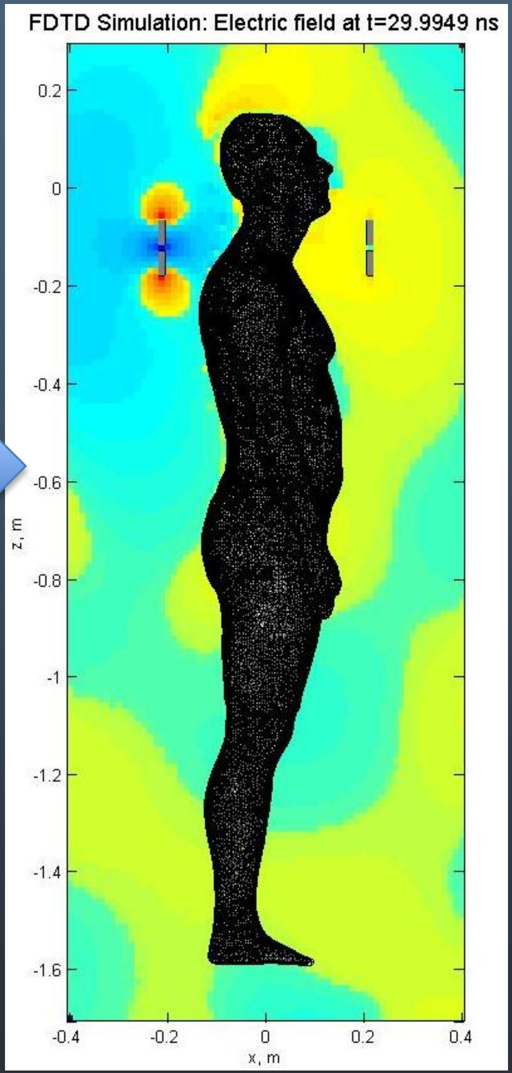

Mesh variations

A variety of body positions are available.

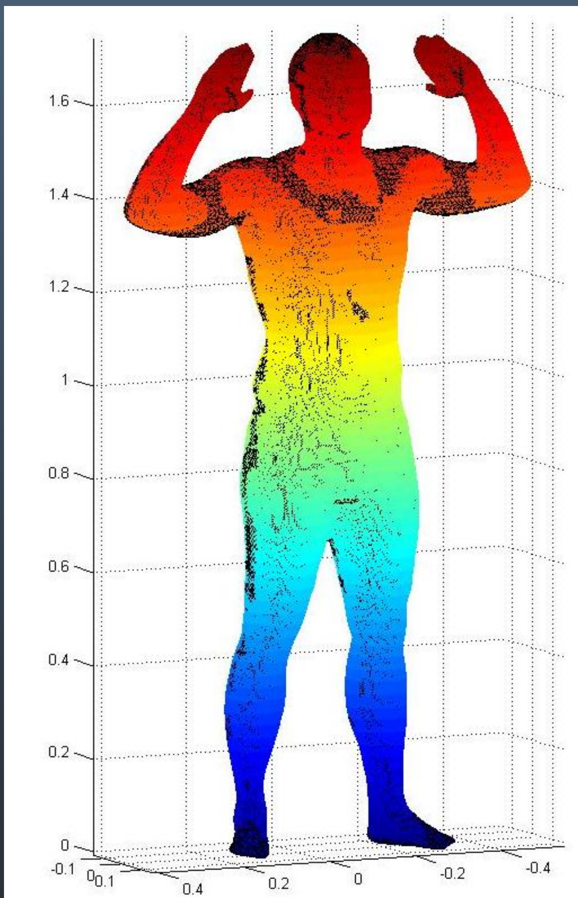

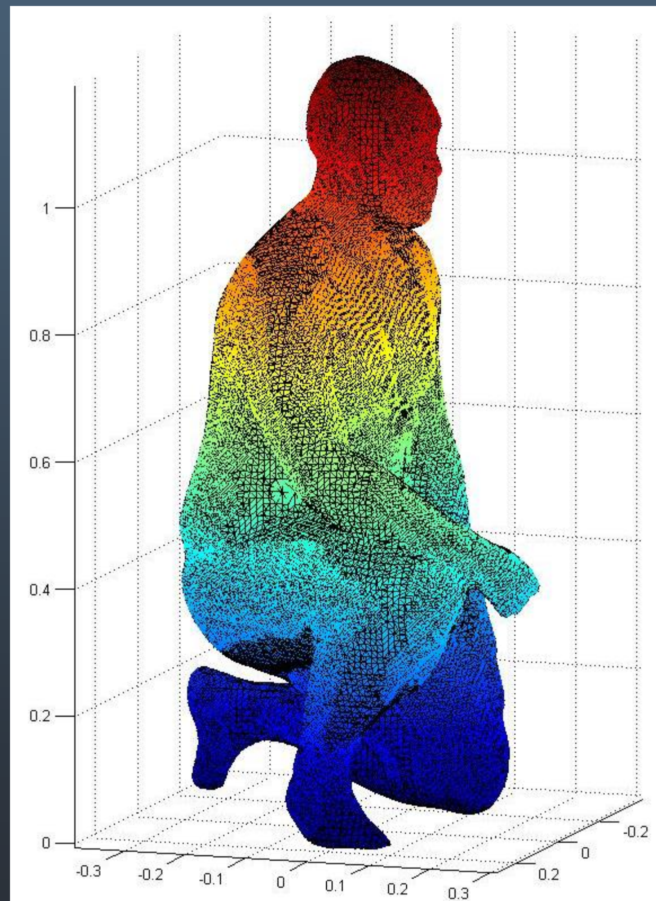

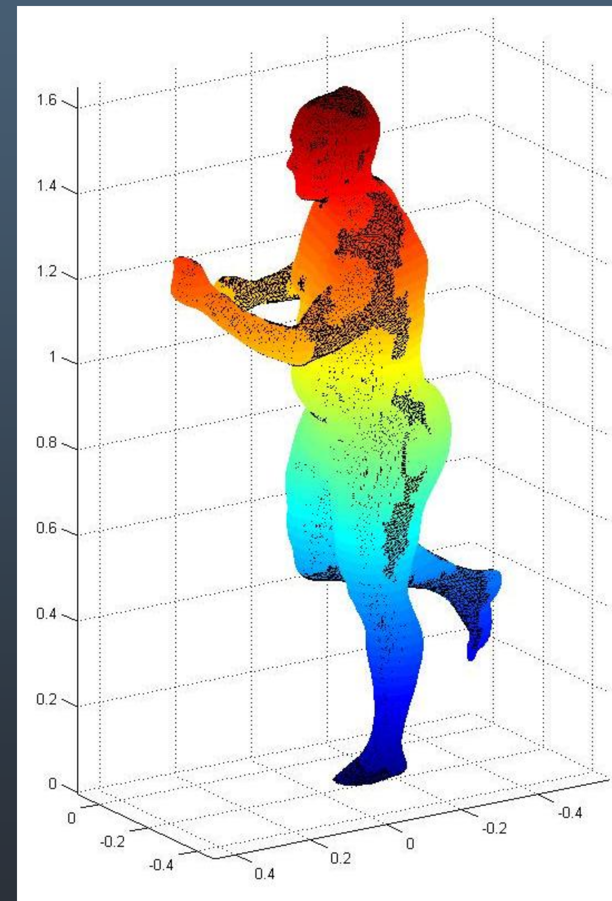

Human phantoms-torso digitization

- Image of torso and digital representation after 3D scanning.
- Phantom provided by The Phantom Laboratory

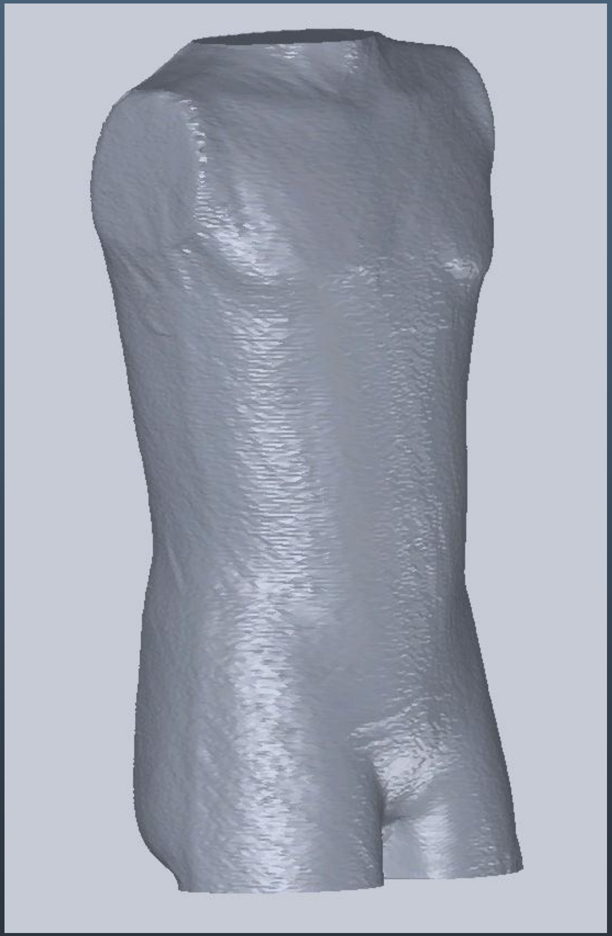

Torso mesh

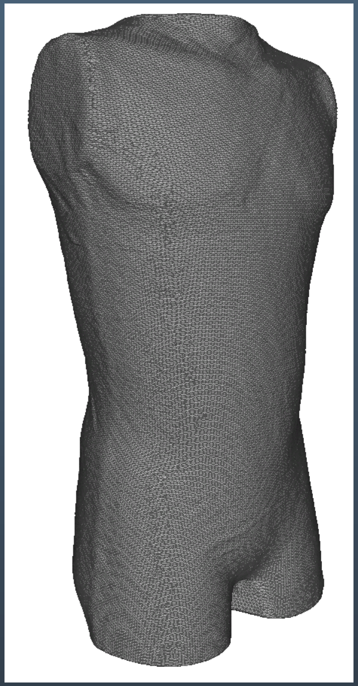
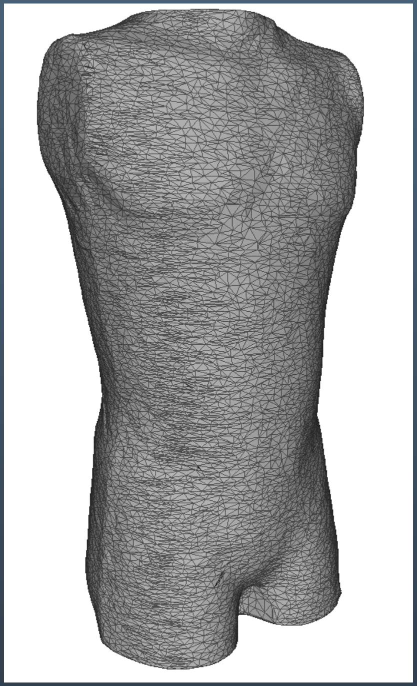
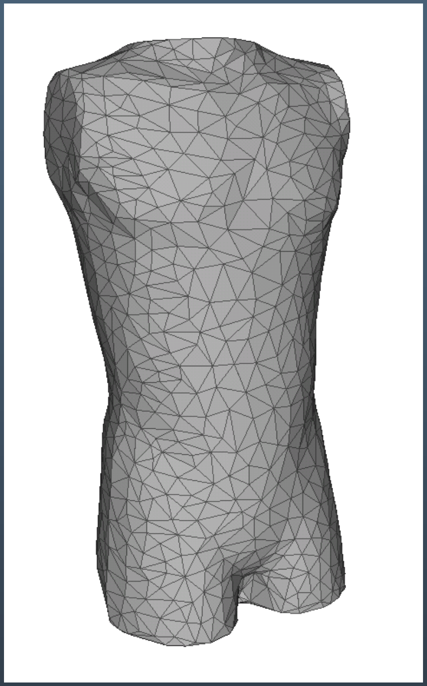
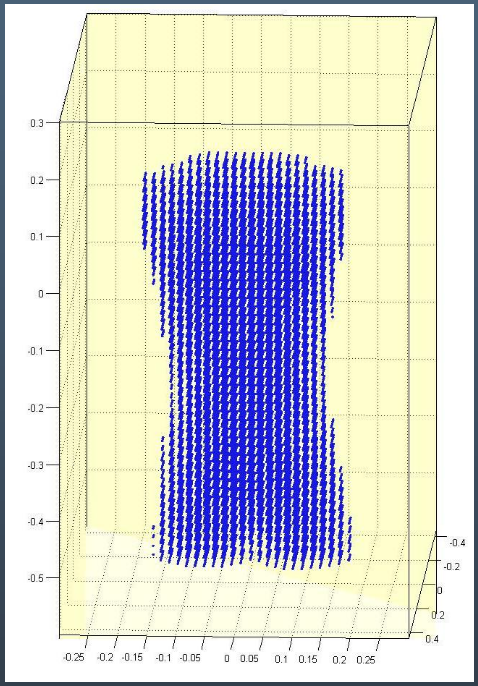

Case Designation	Vertices	Faces
Original	60,005	120,002
Reduction1	12,003	24,000
Reduction2	1,202	2,400

A near-field scanning array – torso

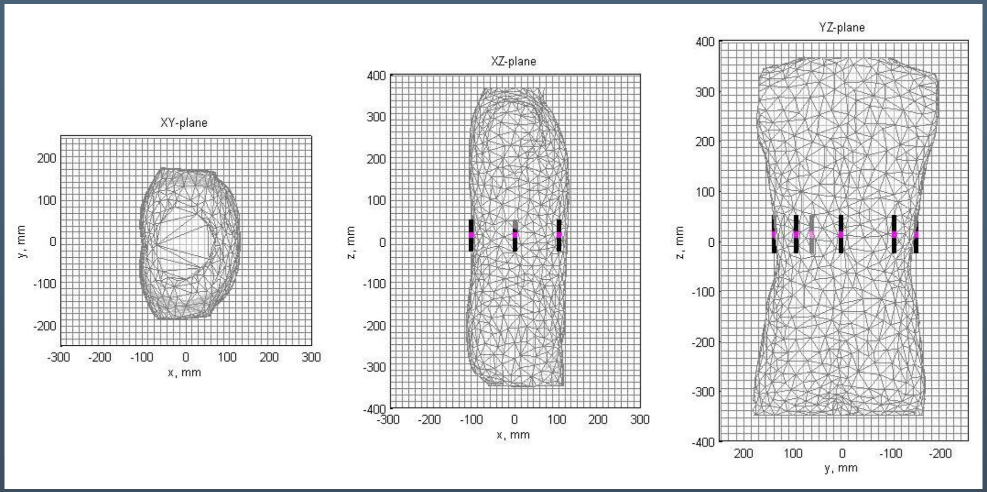

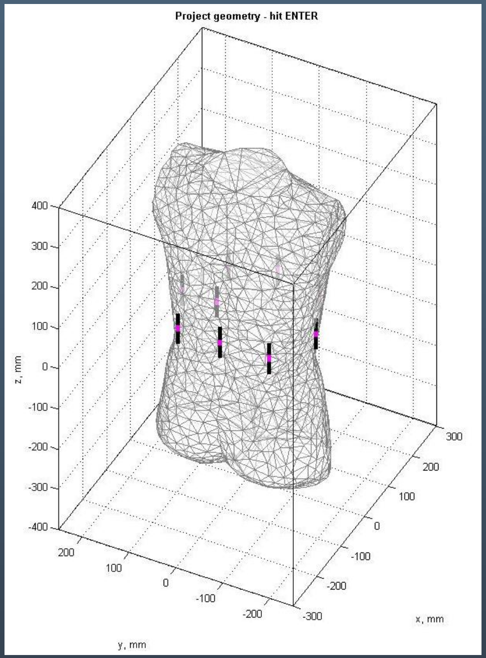

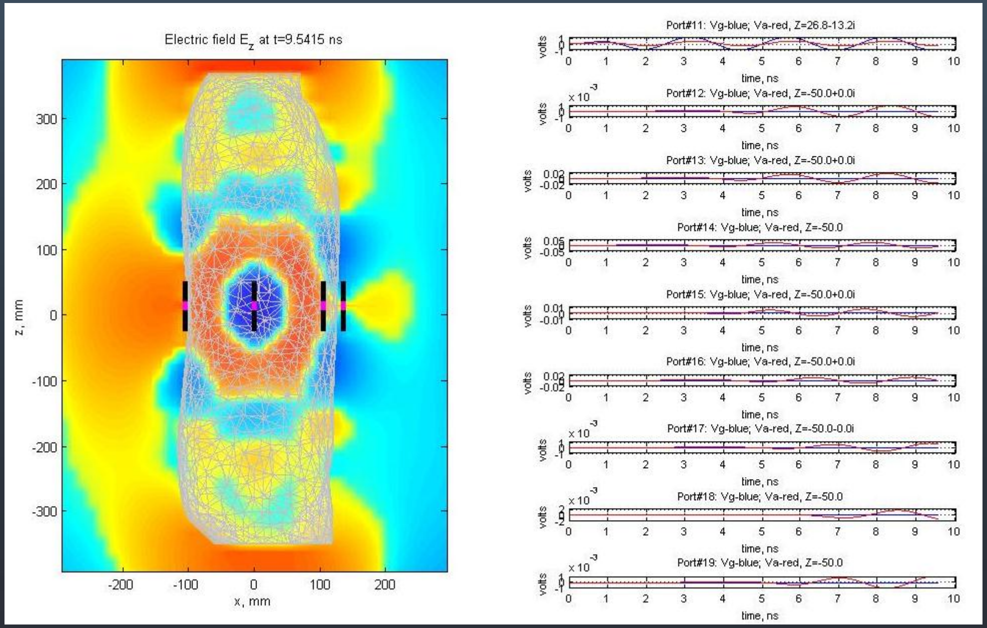

- 1x8 dipole array
- Homogeneous body
- Near-field scanning array task: ~2λ x 2λ x 2λ domain

Human phantoms - head

Phantom from The Phantom Laboratory

Head mesh

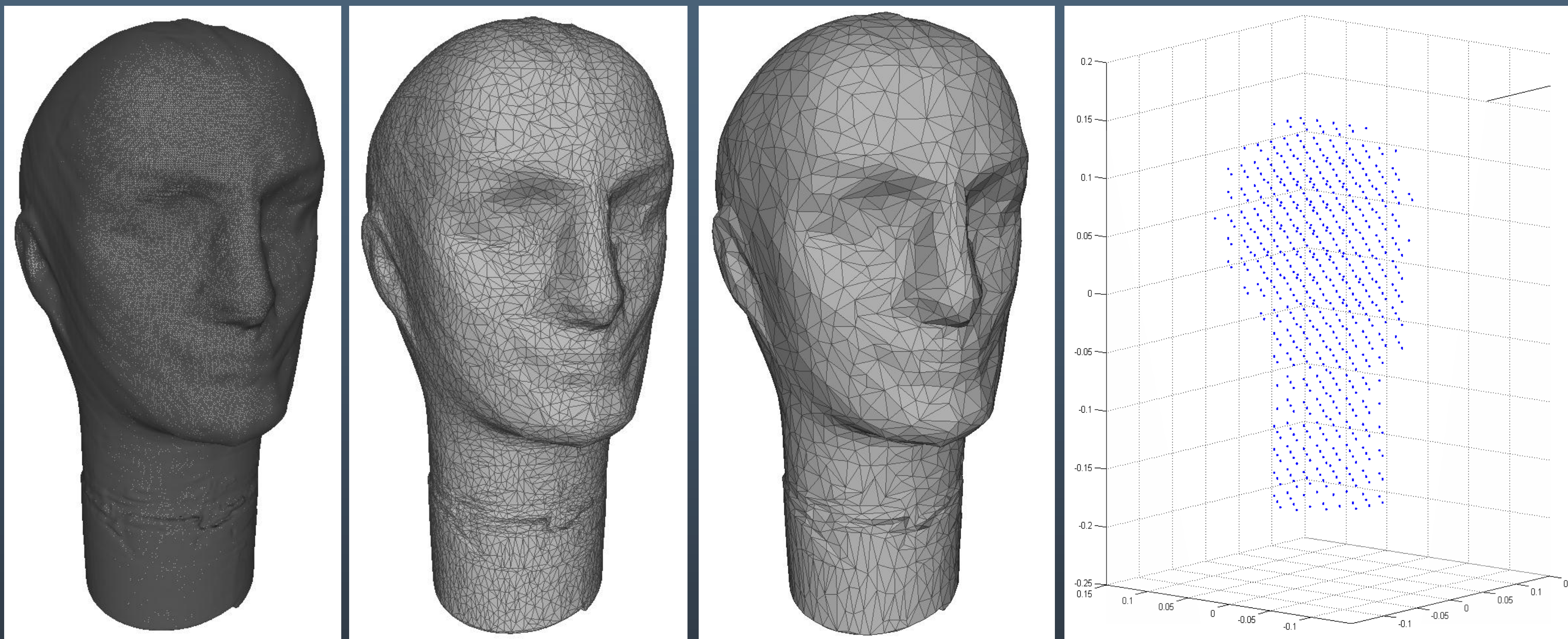

Case Designation	Vertices	Faces
Original	297,149	594,490
Reduction1	8,918	17,832
Reduction2	2,229	4,458

A near-field scanning array – head

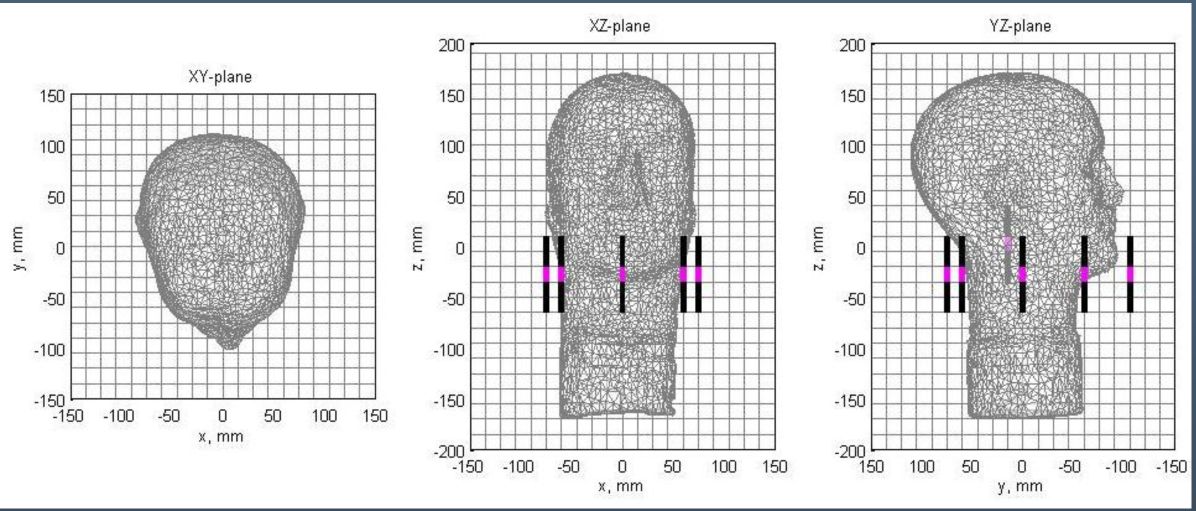

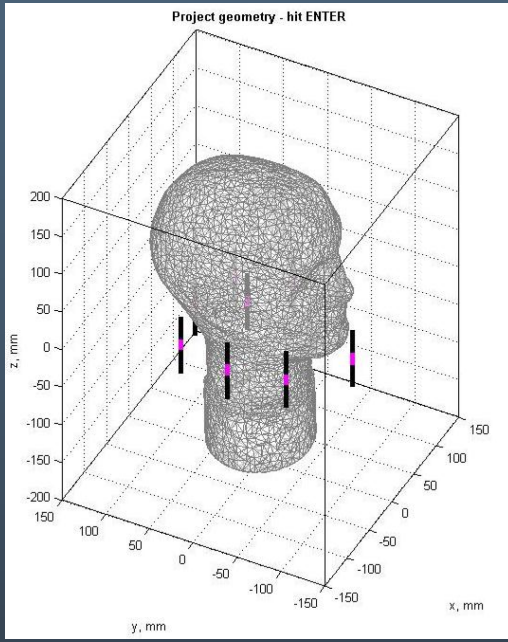

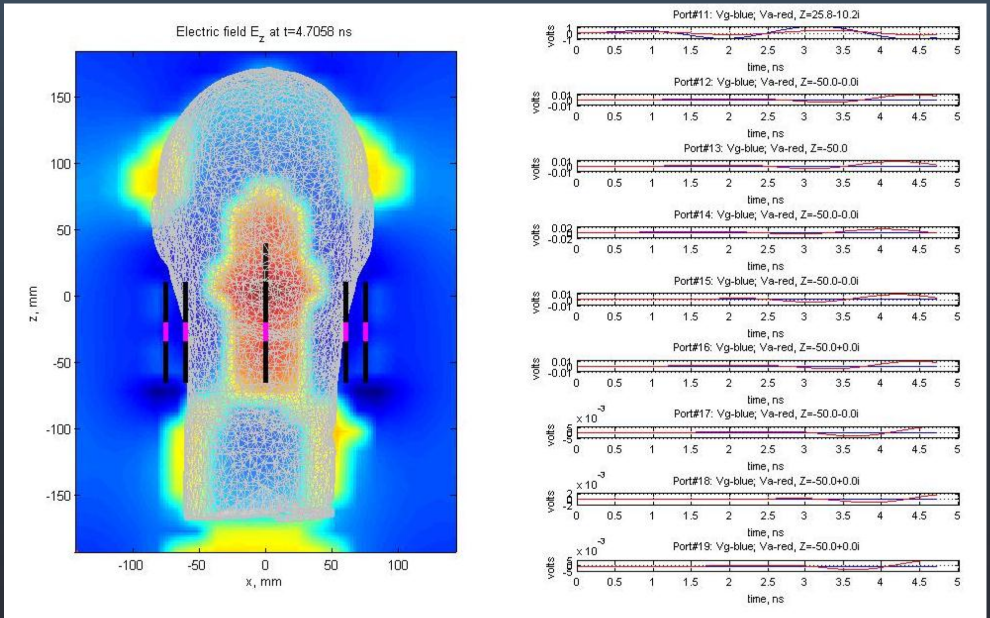

- 1x8 dipole array
- Homogeneous body
- Near-field scanning array task: ~2λ x 2λ x 2λ domain

A near-field scanning array – kneeling human

- 1x8 dipole array
- Homogeneous body
- Near-field scanning array task: ~2λ x 2λ x 2λ

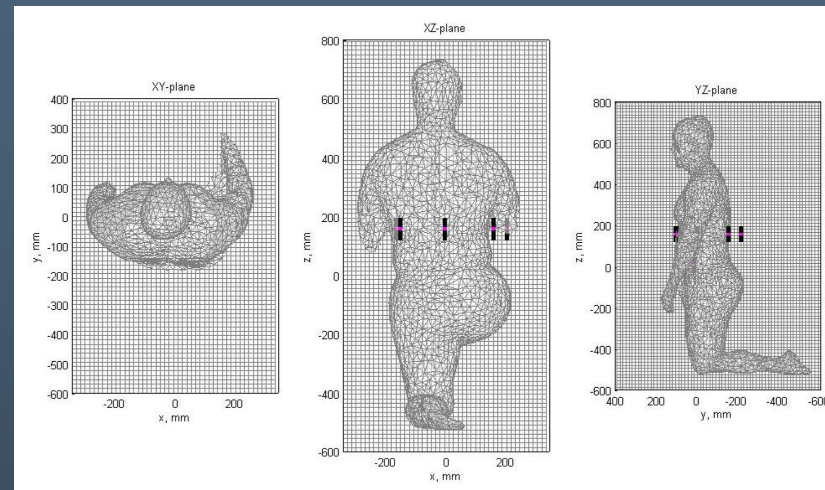

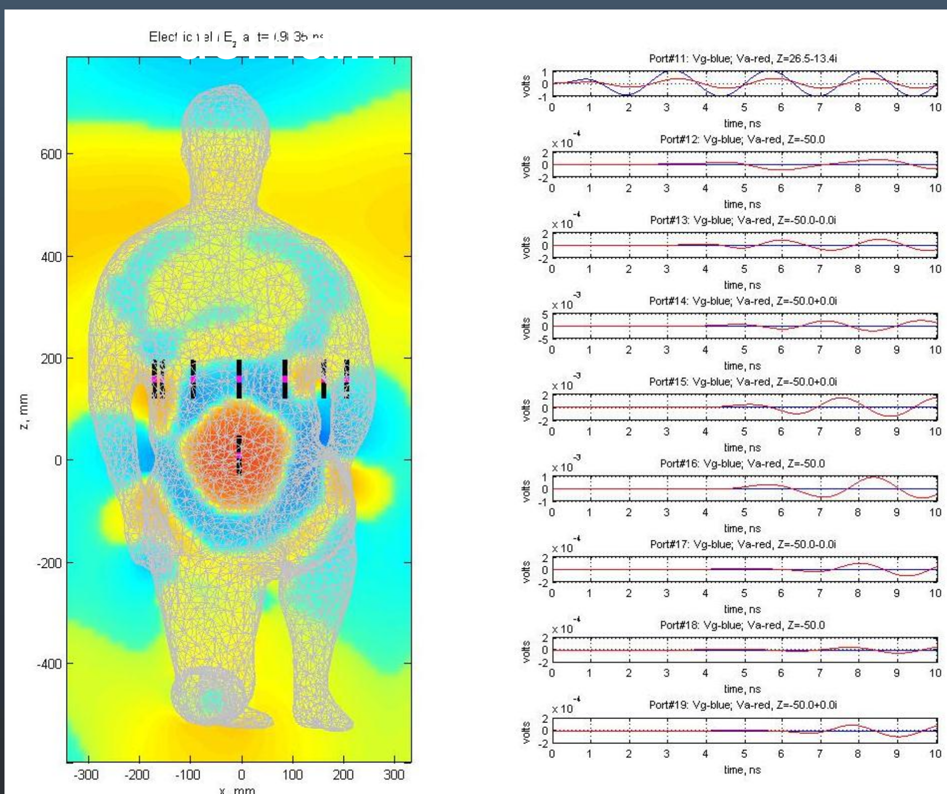

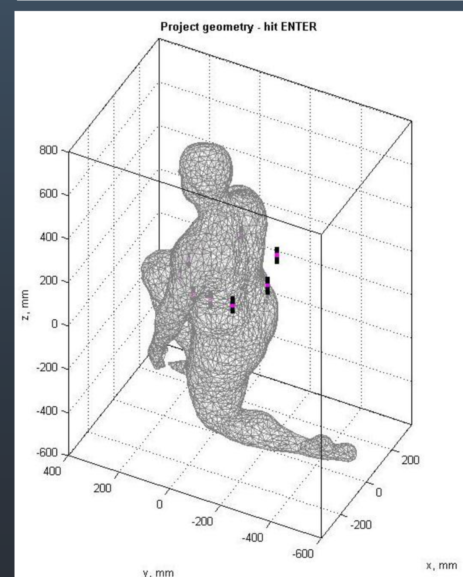

Continued work

Several tasks are either planned or currently being worked:

- Scanning of body phantoms with organs
- Coupling of analytical, experimental and numerical results
- Speeding up the code/increasing accuracy
- Implementing parallel MATLAB engine
- Potential construction of antennas with a focusing element designed for human body near-field scanning
- 1st Workshop on Emerging Body Area Network Technology and Applications (June 19-20, 2011 at WPI, Worcester, MA)

http://www.cwins.wpi.edu/workshop11/index.html

http://www.nist.gov/healthcare/emerging/body-network-workshop.cfm

Acknowledgments

The authors would like to thank:

- Mr. Jeremy Carson of the U.S. Army Natick Soldier Research, Development & Engineering Center for his assistance in use of the 3D body scanner and his invaluable advice on manipulation of the resulting data sets
- Mr. Luigi Giaccari for access to and use of his MATLAB scripts *InPolyedron.m* and *MyRobustCrust.m*. These are both essential pieces to the generation of our custom FDTD meshes

This work was partially supported by NIST grant "RF propagation, measurement, and modeling for wireless body area networking" (PI – K. Pahlavan, ECE, WPI)

Appendix A: Effect of body proximity on a small dipole

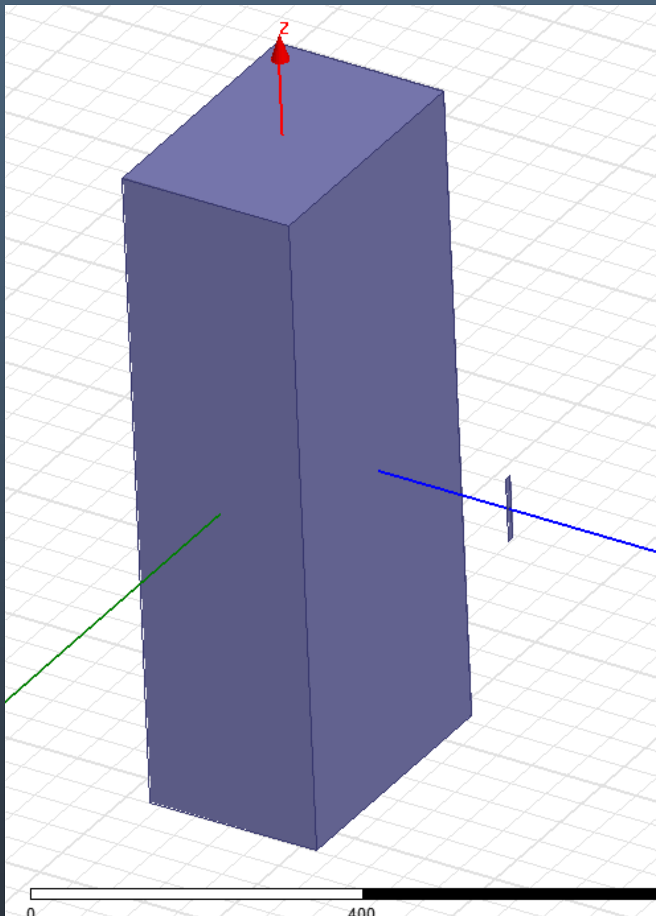

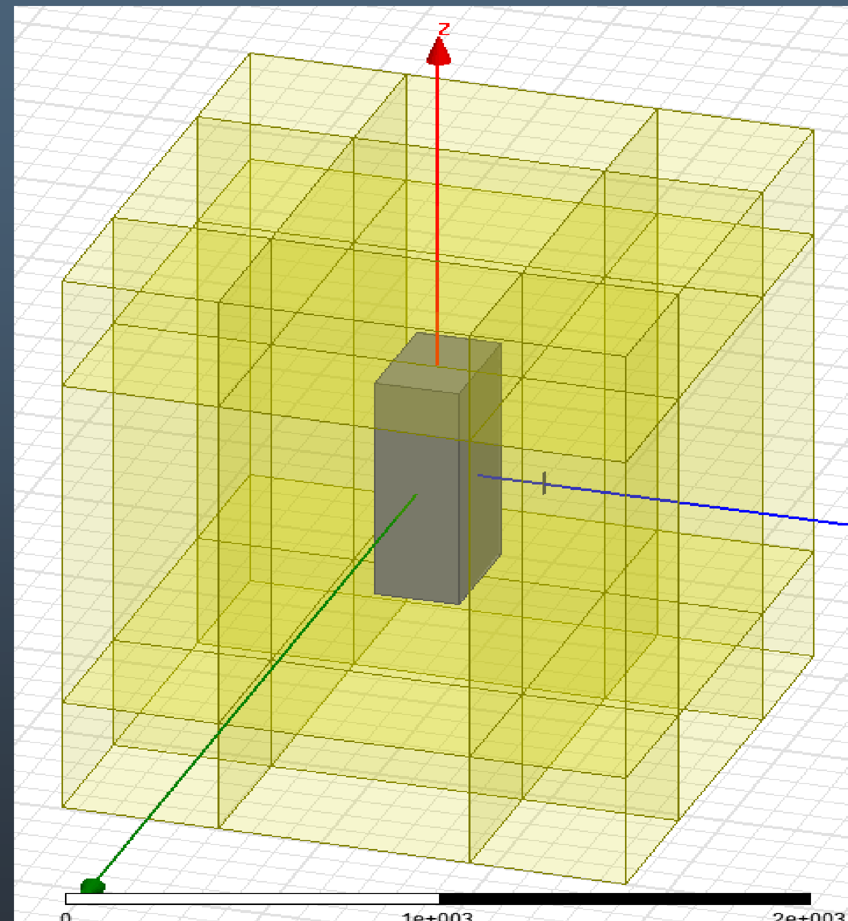

Establish input impedance base – one element

Impedance results

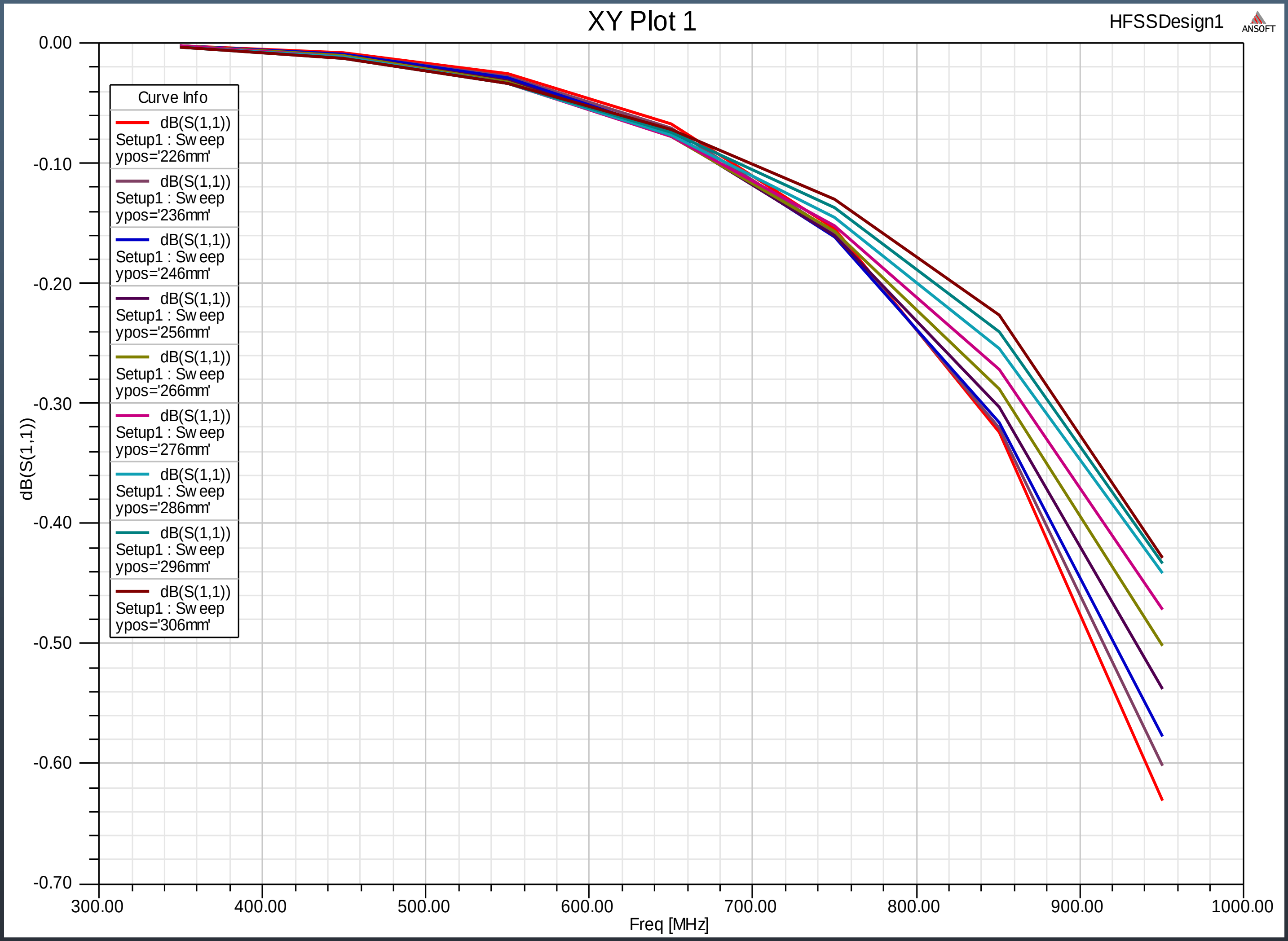

Appendix B: Internal antenna study

The ‘human body’ under consideration is modeled as a 20 cm x 40 cm x 90 cm block of homogeneous material. Simulation of two dielectric constants is underway:

- $\varepsilon_r = 40$
- $\varepsilon_r = 50$

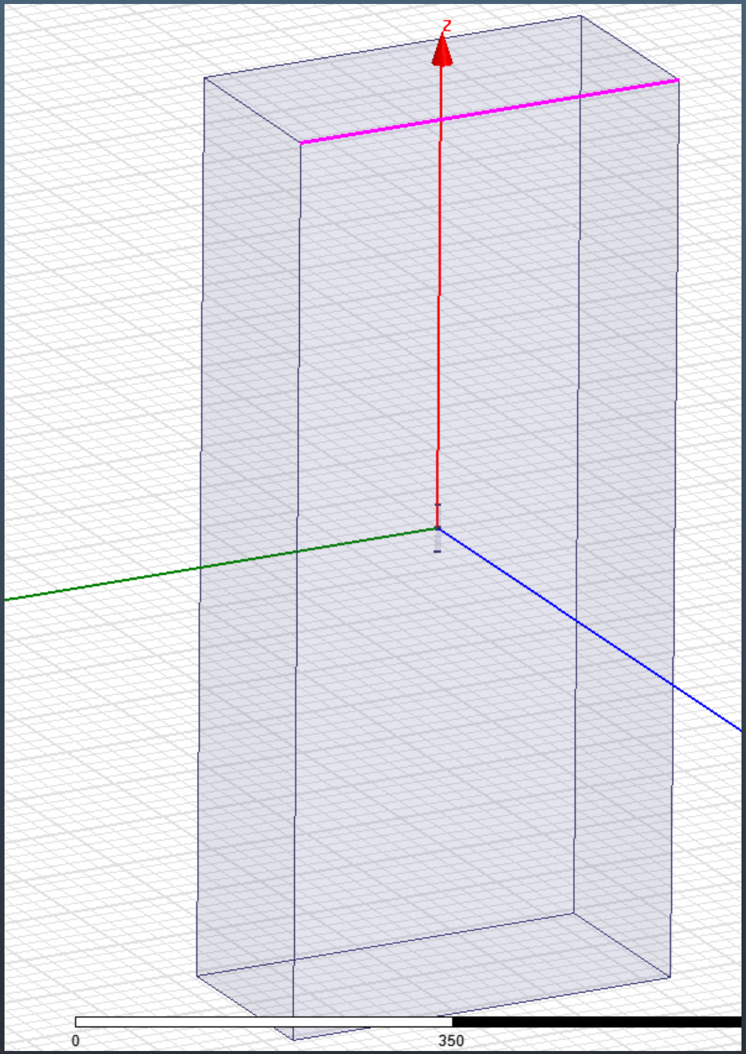

ANSOFT antenna model

A model of a cylindrical dipole antenna has been inserted into the center of a block representing the human body. The dipole has the following parameters:

- Radius = 5 mm
- Feed = 5 mm x 3 mm
- Total varies from 15 mm to 100 mm

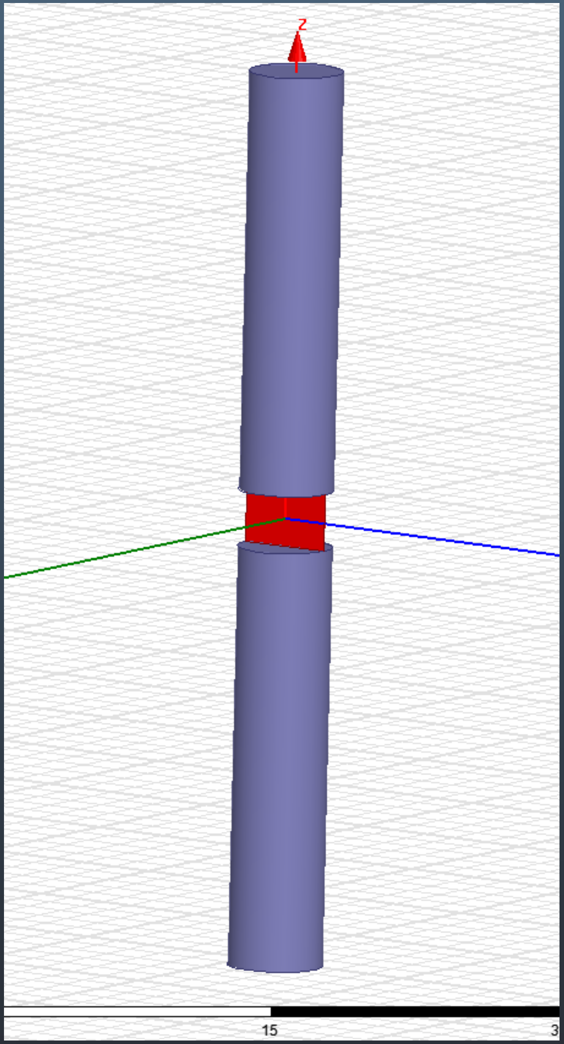

Reflection coefficient

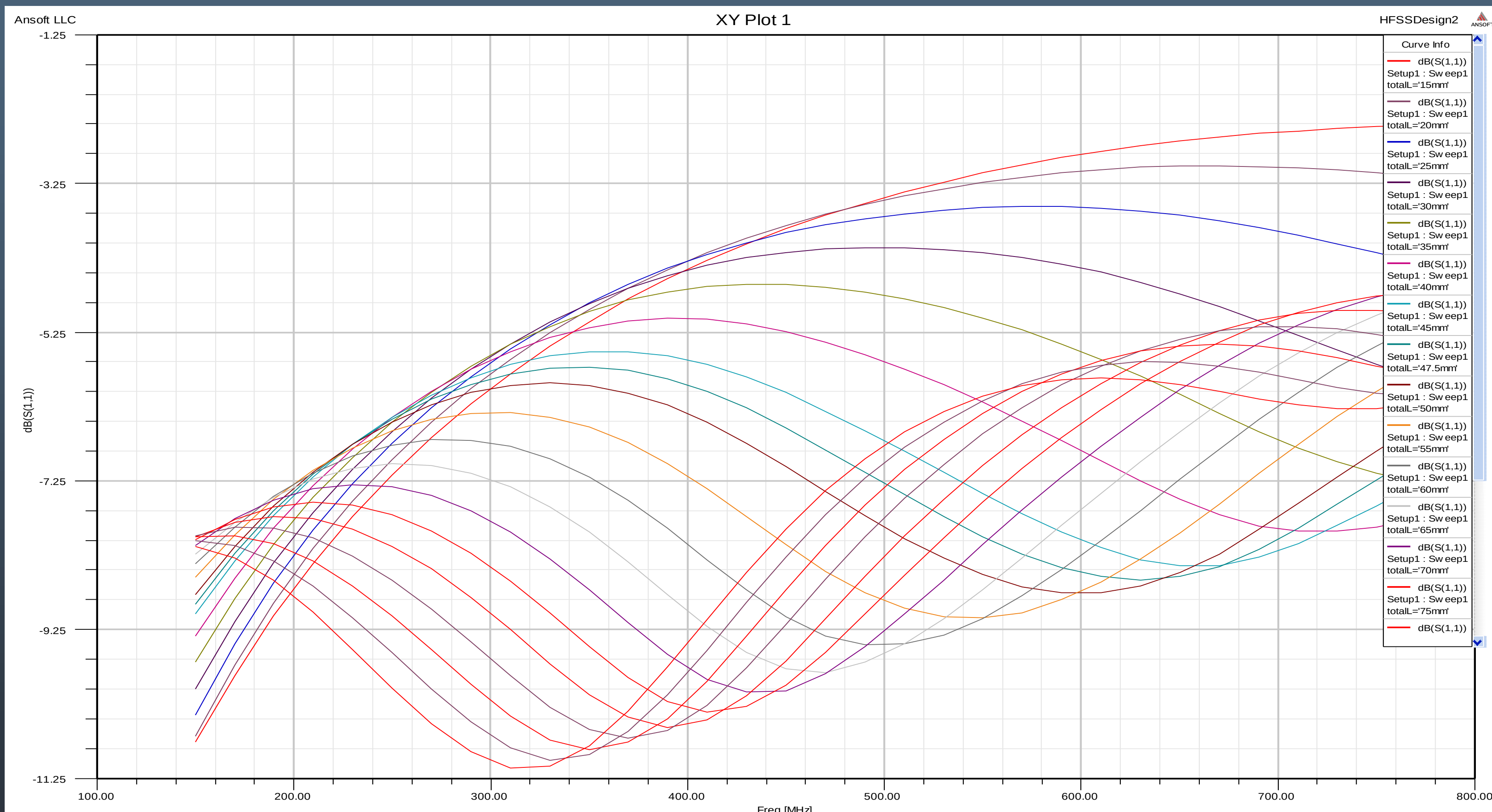

When $\varepsilon_r = 40$, the reflection coefficients across the parametric length study are shown above. These show several candidates with suitable characteristics across the frequency band of interest.

Reflection coefficient

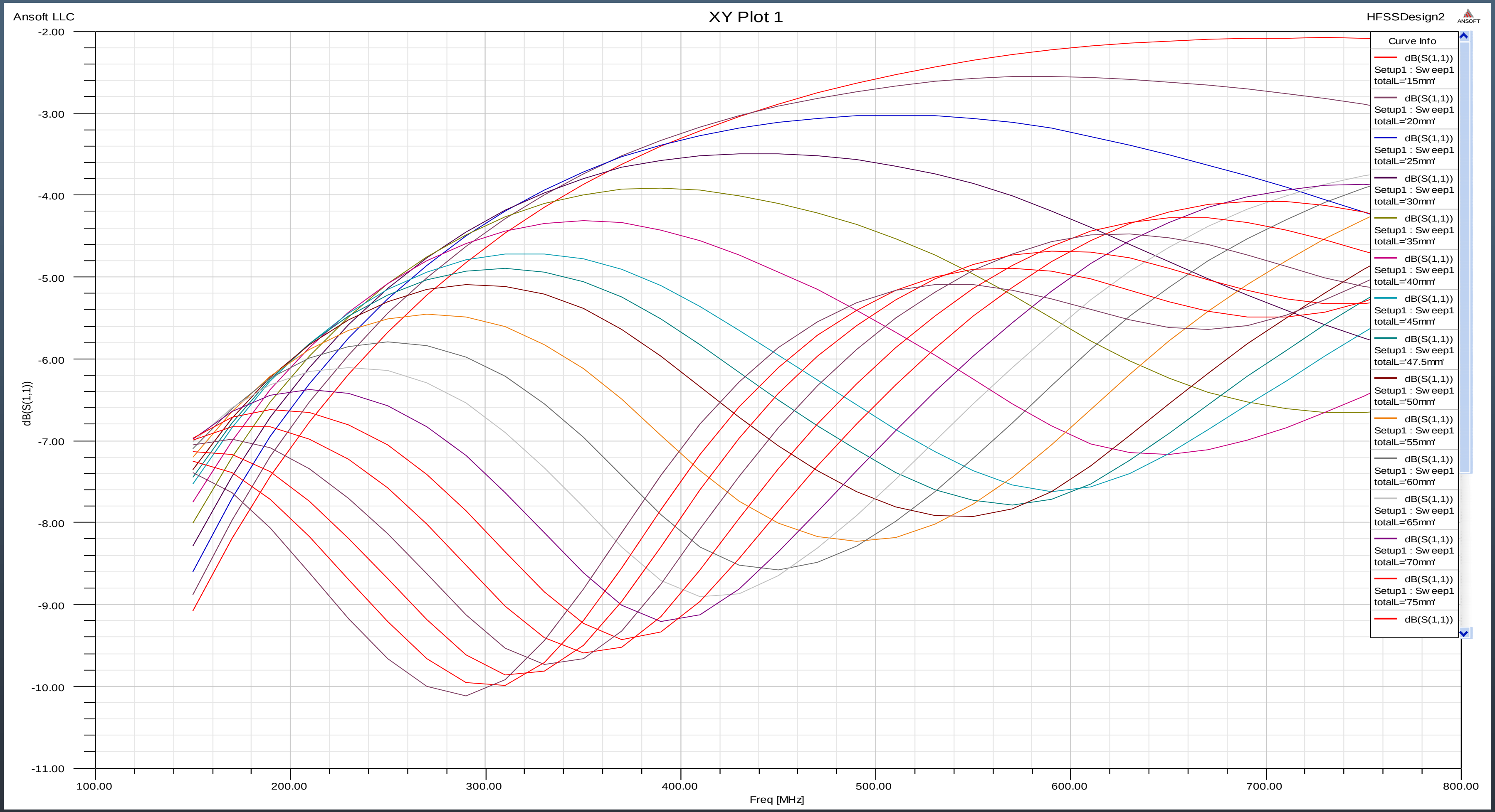

When $\varepsilon_r = 50$, the reflection coefficients for the parametric length study are shown above. These are slightly higher than in the case of $\varepsilon_r = 40$ but show the same general behavior.

Electric fields

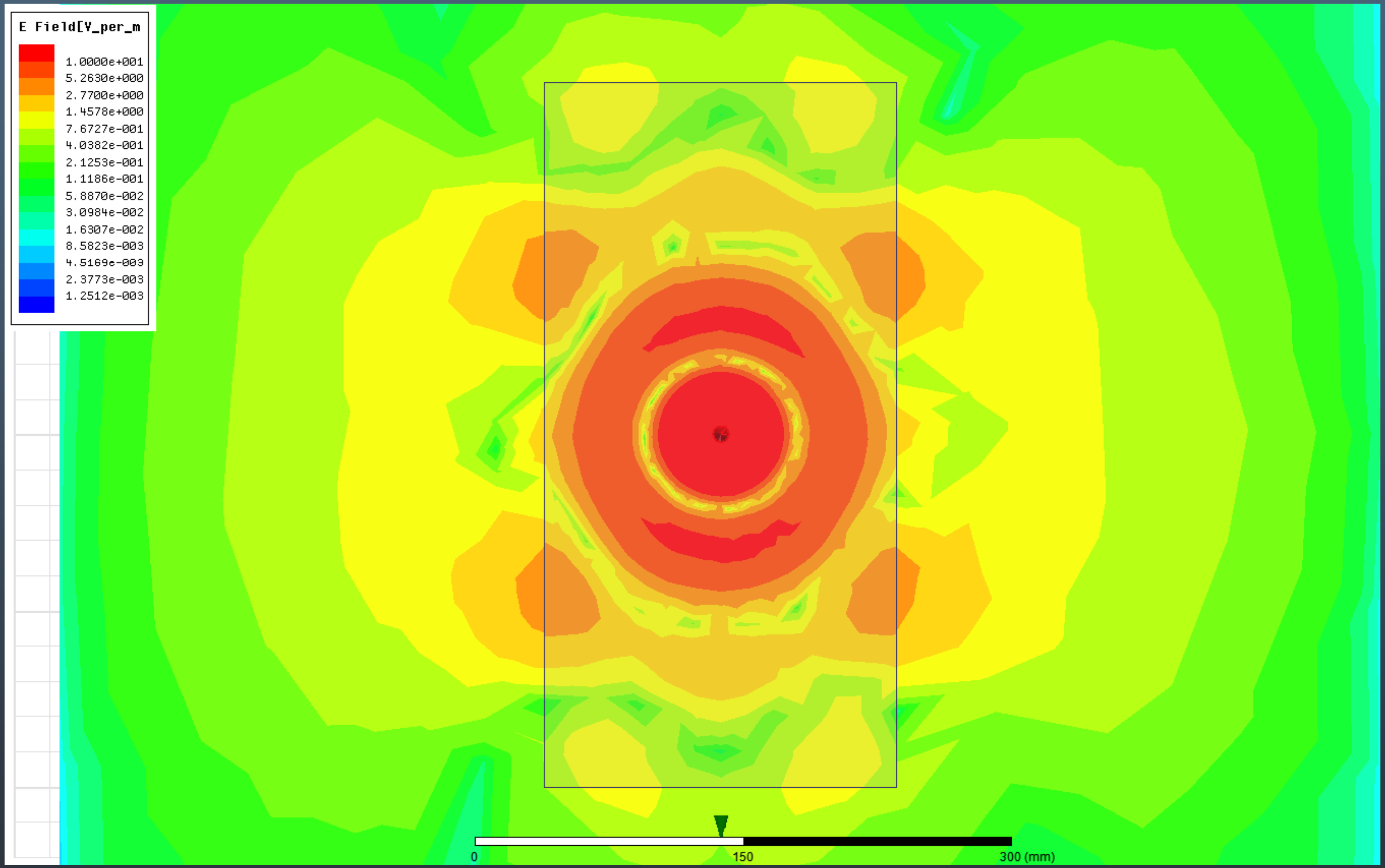

As one looks at the body from the top, concentric Electric Field rings become apparent and radiate out from the antenna source. Hot spots appear at various locations.